AD_____

Award Number: W81XWH-08-1-0574

TITLE: Chemical Agonists of the PML/Daxx Pathway for Prostate Cancer Therapy

PRINCIPAL INVESTIGATOR: Dr. John Reed

CONTRACTING ORGANIZATION: Burnham Institute for Medical Research
La Jolla, CA 92037

REPORT DATE: April 2011

TYPE OF REPORT: Final

PREPARED FOR: U.S. Army Medical Research and Materiel Command
Fort Detrick, Maryland 21702-5012

REPORT DOCUMENTATION PAGE

Form Approved
OMB No. 0704-0188

1. REPORT DATE *(DD-MM-YYYY)*	**2. REPORT TYPE**	**3. DATES COVERED** *(From - To)*
01-04-2011	Final	15 AUG 2008 -31 MAR 2011

4. TITLE AND SUBTITLE

Chemical Agonists of the PML/Daxx Pathway for Prostate Cancer Therapy

5a. CONTRACT NUMBER

5b. GRANT NUMBER
W81XWH-08-1-0574

5c. PROGRAM ELEMENT NUMBER

6. AUTHOR(S)

Dr. John Reed

E-Mail: mhanaii@sanfordburnham.org

5d. PROJECT NUMBER

5e. TASK NUMBER

5f. WORK UNIT NUMBER

7. PERFORMING ORGANIZATION NAME(S) AND ADDRESS(ES)

Burnham Institute for Medical Research
La Jolla, CA 92037

8. PERFORMING ORGANIZATION REPORT NUMBER

9. SPONSORING / MONITORING AGENCY NAME(S) AND ADDRESS(ES)

U.S. Army Medical Research and Materiel Command
Fort Detrick, Maryland 21702-5012

10. SPONSOR/MONITOR'S ACRONYM(S)

11. SPONSOR/MONITOR'S REPORT NUMBER(S)

12. DISTRIBUTION / AVAILABILITY STATEMENT

Approved for Public Release; Distribution Unlimited

13. SUPPLEMENTARY NOTES

14. ABSTRACT

Metastatic, hormone refractory prostate cancer is currently an incurable disease. Consequently, novel therapeutic agents are needed that promote killing of malignant prostate cancer cells in a more efficient, less toxic manner. The goal of this project was to identify chemicals that activate an endogenous anti-cancer mechanism that induces tumor cell suicide and auto-destruction. To achieve this goal, we focused on an intrinsic tumor suppressor system involving the proteins PML and Daxx, which control the activity of the genome and render tumor cells more vulnerable to cell death. We devised robotic automated screening methods that permited us to test a collection of chemicals in search of molecules with the proper characteristics to activate the PML/Daxx tumor suppressor pathway in hormone refractory prostate cancer cells. The chemicals identified provide a starting point for futher optimization with respect to their chemical structures so that they are potent and have the proper behavior in the body to reach tumor cells at effective concentrations. Altogether, these efforts provide a foundation for innovative new experimental therapeutics for advanced prostate cancer.

15. SUBJECT TERMS

PML, Daxx, Prostate

16. SECURITY CLASSIFICATION OF:			**17. LIMITATION OF ABSTRACT**	**18. NUMBER OF PAGES**	**19a. NAME OF RESPONSIBLE PERSON**
a. REPORT	**b. ABSTRACT**	**c. THIS PAGE**			USAMRMC
U	U	U	UU	26	**19b. TELEPHONE NUMBER** *(include area code)*

Standard Form 298 (Rev. 8-98)
Prescribed by ANSI Std. Z39.18

Table of Contents

Page

INTRODUCTION

PML Oncogenic Domains (PODs) are nuclear structures where specific proteins concentrate, including PML, a tumor suppressor (1, 2). The PML protein is the primary structural component of PODs, also known as PML-NBs (PML-Nuclear Bodies), ND-10, or Kremer bodies (1). Cells derived from *pml*-/- embryos exhibit broad resistance to a wide range of apoptotic stimuli, suggesting that this protein somehow sets apoptosis thresholds in mammalian cells (3). Interestingly, several viral proteins have been reported to interfere with POD formation, while interferons promote POD formation, suggesting an important role for these nuclear structures in host defense against viruses (4-9). Since many viruses possess mechanisms for blocking apoptosis of infected cells as a mechanism for parasitizing cellular hosts for purposes of producing virus, these observations may be connected to the role of PODs in modulating apoptosis sensitivity. Several proteins have been identified that target to PODs, some of which interact PML. Among these proteins is Daxx, a pro-apoptotic protein of unclear mechanism. Targeting of Daxx to PODs and its interaction with PML is inducible by interferons and arsenicals, correlating with increased apoptosis, and possibly explaining in part the therapeutic benefit of these agents in the treatment of selected types of leukemia and cancer (1, 2). Also, siRNA-mediated ablation of Daxx expression or expression of dominant-negative mutants of Daxx can suppress apoptosis induction by specific types of cell death stimuli, in human epithelial tumor cell lines (5, 10). Daxx functions as a transcriptional repressor, binding histone deacetylases (HDACs) and DNA methyltransferases. Of specific relevance to apoptotic mechanisms, our laboratory discovered that Daxx associates with Rel-B, a transcription factor of the NF-κB family that directly controls the expression of numerous anti-apoptotic genes, including cIAP2, cFLIP, Bfl-1 (A1), and others (11). Thus, Daxx silences these anti-apoptotic Rel-B target genes, promoting an apoptosis-sensitive state. We hypothesized that chemical compounds that induce POD formation in prostate cancer cells would promote apoptosis, providing a new type of experimental therapeutic for hormone refractory prostate cancers. Furthermore, we hypothesized that by undertaking chemical library screening using high-content imaging methods to monitor PML and Daxx protein targeting to PODs, it would be possible to identify compounds that offer distinct advantages over the currently known POD-inducers (arsenicals and interferons). To this end, we assembled a multi-disciplinary team of scientists (including cell and molecular biologists, medicinal chemists, and engineers) to test these hypotheses. A summary of our progress after nearly one year of effort is provided herein.

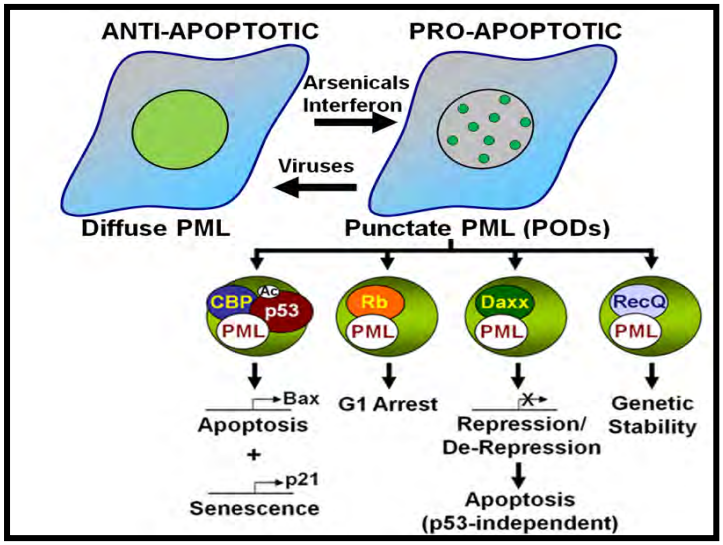

Figure 1. ***PML localization to PODs regulates the assembly and function of proteins involved in tumor suppression.*** PML is required for CBP-mediated acetylation (Ac) of p53. Acetylation increases p53-mediated transcription of Bax and p21. PML may be required for Rb-induced G1 arrest. Daxx represses anti-apoptotic protein expression at PODs, promoting p53-independent apoptosis. Daxx localization to PODs favors PTEN nuclear localization, which may also induce G1 arrest. PML is required for genetic stability, and interacts with proteins such as RecQ DNA helicase.

BODY

We excellent progress towards meeting the objectives of the funded project. A brief summary for each task is provided here with a description of the accomplishments.

Task #1. Devise HTS assays for identification of compounds that induce Daxx recruitment into PODs.

This goal was accomplished, except that we decided to track PMLs targeting to PODs rather than Daxx because PML anchors the entire complex and because PML yielded a superior compared to Daxx. We generated a high content screening (HCS) assay for compound library screening that measures the

localization of PML to PODs by immunofluorescence. To achieve this goal, we first verified that we could monitor the localization of PML and Daxx to nuclear PODs following stimulation of a tumor cell line with interferon. For immunofluorescence-based POD detection, HeLa cells (3150 cells/well, 50 µL volume) were seeded overnight in clear-bottom 384-well plates (190 µm thick optically clear plastic bottom). Cells were then treated with 2 U/µL IFN-γ for 12 h, fixed, and stained with the nuclear DAPI stain, a mouse monoclonal anti-PML antibody (Santa Cruz Biotechnology), and an Alexa Fluor 488 chicken anti-mouse antibody (Invitrogen). Imaging was performed using the Beckman Coulter Cell Lab IC-100 Image Cytometer. IFN-γ-induced PML localization to PODs was clearly visible (Figure 1), as we have previously shown (5). Increasing IFN-γ concentration beyond 2 U/µL did not visibly increase POD formation, and POD formation was more visible with IFN-γ than with As_2O_3 (data not shown; quantified dose-response curve shown on Figure 1).

To confirm POD formation, the aforementioned experiment was performed again, but with dual PML (mouse monoclonal anti-PML primary and Alexa Fluor 488 chicken anti-mouse secondary antibody) and Daxx (rabbit polyclonal anti-Daxx primary and Alexa Fluor568 goat anti-rabbit secondary antibody) staining. Indeed, PML and Daxx co-localize to punctate areas within nuclei, and the number of these punctate areas increases with IFN-γ treatment (Figure 2).

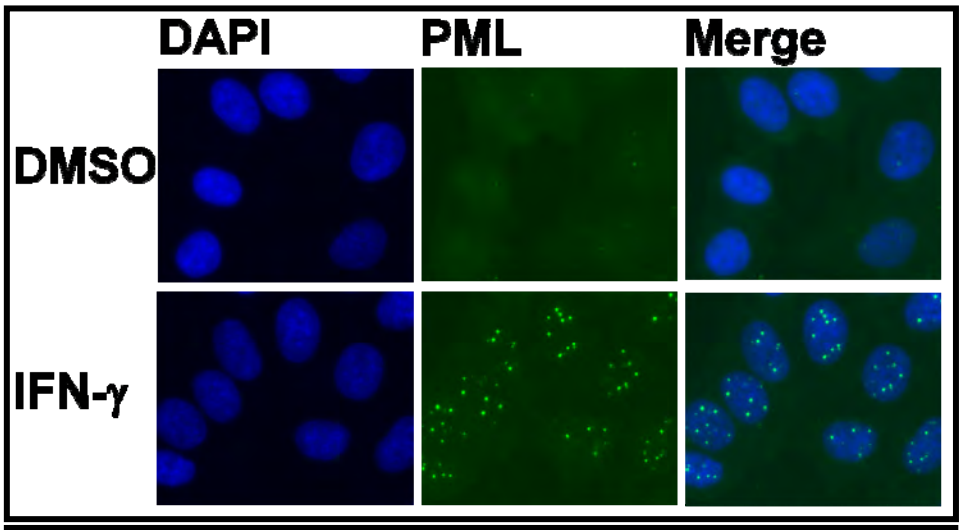

Figure 1. ***PML localizes to PODs after IFN-γ treatment.*** HeLa cells were seeded in 384-well plates, treated (12 h) with DMSO (0.1%) or IFN-γ (2 U/µL), immunostained with mouse monoclonal anti-PML and Alexa Fluor 488 chicken anti-mouse antibodies (1:200 dilutions; *green*), and incubated in DAPI (nuclear stain; 100 ng/mL; *blue*). Cells were imaged using the Beckman Coulter Cell Lab IC-100 Image Cytometer (40x 0.6NA ELWD Fluor objective).

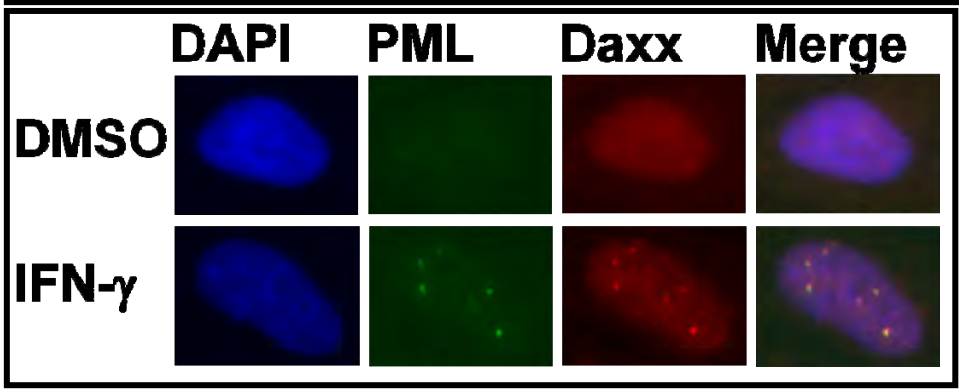

Figure 2. ***PML and Daxx co-localize to PODs after IFN-γ treatment.*** HeLa cells were seeded in 384-well plates, treated (12 h) with DMSO (0.1%) or IFN-γ (2 U/µL), immunostained for PML (mouse monoclonal anti-PML primary antibody, Alexa Fluor 488 chicken anti-mouse secondary antibody; *green*) and Daxx (rabbit polyclonal anti-Daxx primary antibody, Alexa Fluor568 goat anti-rabbit secondary antibody; *red*), and incubated in DAPI (nuclear stain; 100 ng/mL; *blue*). Cells were imaged using the Beckman Coulter Cell Lab IC-100 Image Cytometer (40x 0.6NA ELWD Fluor objective).

To quantify the extent of POD formation (i.e. the number of PODs per cell, the intensity of PML localization, and the fraction of cells per well with extensive numbers of PODs), the "POD detection" algorithm was developed in collaboration with the High Content Screening (HCS) Core within the Burnham Center for Chemical Genomics (BCCG). This algorithm was based on previous work performed in collaboration with Dr. Jeffrey Price and the Burnham team, wherein the translocation of GFP-tagged androgen receptor from cytoplasm to a hyperspeckled pattern within nuclei was quantified (12).

The POD detection algorithm was developed using Beckman Coulter CytoShop (for POD outlining) and MathWorks MATLAB (for ratio threshold optimization) software, but is adaptable to other software packages with fluorescent spot detection algorithms. Firstly, the nuclear ("blue") image (DAPI stain) was used to produce a "nuclear mask", which identified all nuclei in an image (Figure 3). This nuclear mask was applied to the PML ("green") image. All green pixels outside of this nuclear mask were eliminated. Next, PODs were outlined based on the identification of green pixels with higher intensities than their surrounding pixels (using CytoShop's aggregate detection), with the minimum size of a POD defined based on IFN-γ control wells (CytoShop "Object Scale"; Figure 3). This number of detected PODs was then reported on a per-nucleus basis, and used to determine the percentage of nuclei per image that were "POD-positive". The value for number of detected PODs above which a nucleus is considered POD-positive was determined to be 4.0 by iteratively setting increasing threshold values and determining the Z'-factor for each threshold (on control plates).

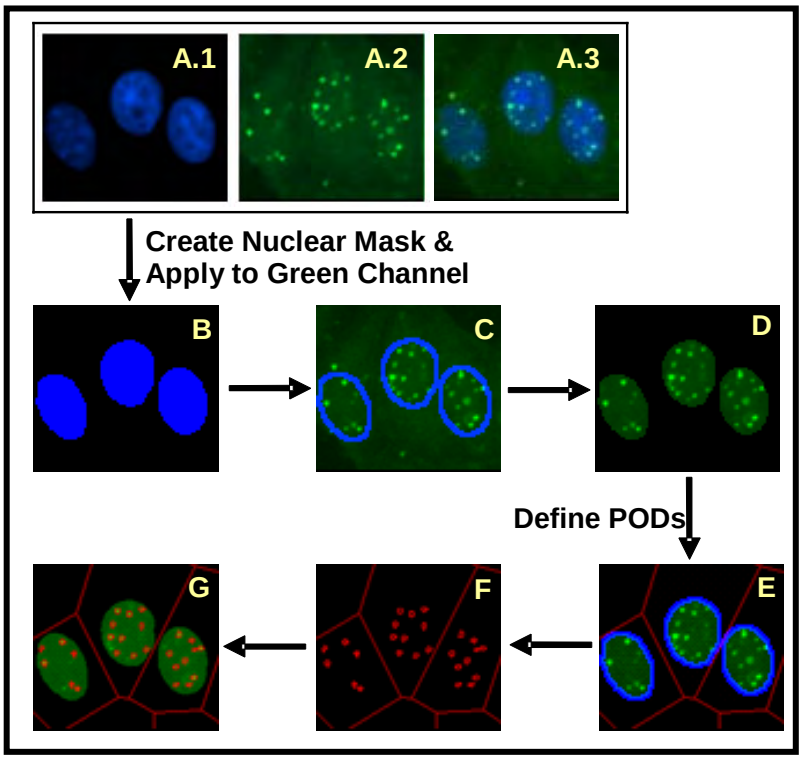

Figure 3. ***Algorithm for detecting PML localization to PODs.*** DAPI (**A.1**; *blue*), PML (**A.2**; *green*), and merged (**A.3**) images of IFN-γ-treated (2 U/μL; 12 h) HeLa cells are shown. **B**, The nuclear (DAPI) image is used to produce a nuclear mask (*blue*). **C**, The nuclear mask (*blue outline*) is applied to the PML image. **D**, Green pixels outside of the nuclear mask are eliminated. **E**, Beckman Coulter CytoShop software is used to estimate cellular area (*red outline*) based on the nuclei. **F**, POD outlines (*red*) are identified based on differences in green pixel brightness. **G**, The number of detected PODs (*red*) is reported on a per-nucleus (*green*) basis. The percentage of POD-positive nuclei (>4.0 PODs per cell) is reported.

To characterize IFN-γ-induced POD formation, HeLa cells were treated with increasing concentrations of IFN-γ, stained for PODs, imaged, and the percentage of POD-positive cells was determined (Figure 4). Manual counting of POD-positive cells confirmed the algorithm-produced quantification (*data not shown*).

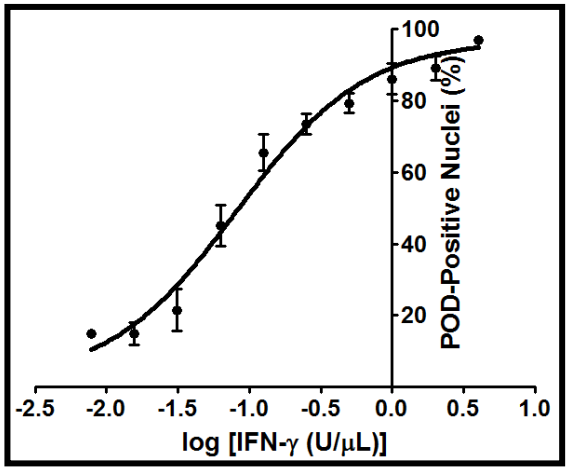

Figure 4. ***Quantification of IFN-γ-induced POD formation.*** HeLa cells were seeded in a 384-well plate (using the ThermoScientific Matrix WellMate liquid dispenser), and treated with increasing concentrations of IFN-γ (12 h) as shown. Cells were immunostained for PODs (mouse monoclonal anti-PML and Alexa Fluor 488 chicken anti-mouse antibodies; 1:200 dilutions), incubated in DAPI (nuclear stain; 100 ng/mL), imaged using the Beckman Coulter Cell Lab IC-100 Image Cytometer (40x 0.6NA ELWD Fluor objective), and quantified using the algorithm described in the text. Mean ± standard deviation are shown (n=4 wells/data point).

CytoShop analyzes cell count, DNA content (based on DAPI-staining intensity), and nuclear shape. Wells with aberrations (e.g. 3 standard deviations from the mean) in these categories will be flagged and the images will be manually examined.

To evaluate the HTS readiness of the HCS, statistical characterization of the assay was performed. Cells were seeded onto 384-well plates using the ThermoScientific Matrix WellMate liquid dispenser, and positive and negative controls were added with the Beckman Coulter Biomek FX Laboratory Automation

Workstation. Cells were then immunostained with the Titertek MAP-C, imaged with the Beckman Coulter Cell Lab IC-100 Image Cytometer using a 40x 0.6NA ELWD Fluor objective, and the images processed. From these experiments, we determined the Z'-factor using the equation: Z'-Factor = 1 - $(3\sigma_{positive} + 3\sigma_{negative}) / |(\mu_{positive}-\mu_{negative})|$, where $\sigma_{positive}$ is the standard deviation of the positive control, $\sigma_{negative}$ is the standard deviation of the negative control, $\mu_{positive}$ is the mean of the positive control, and $\mu_{negative}$ is the mean of the negative control.

In a preliminary experiment (Figure 5), we determined the Z'-factor, using IFN-γ (2 U/μL) as a positive control and DMSO (0.1%) as a negative control (n=11 wells per condition), to be 0.63. In a more complete experiment (Figure 6), we determined the Z'-factor, using IFN-γ (2 U/μL) as a positive control and DMSO (0.1%) as a negative control (n=100 wells per condition), to be 0.64. Using IFN-γ (2 U/μL) as a positive control and no treatment as a negative control (n=100 wells per condition), the Z'-factor is 0.65 (Figure 6). In any case, the consistent results suggest a highly reproducible HCS that is minimally affected by a concentration of DMSO typically used for screening. This assay was reproducible in final DMSO concentrations of up to 1% (data not shown).

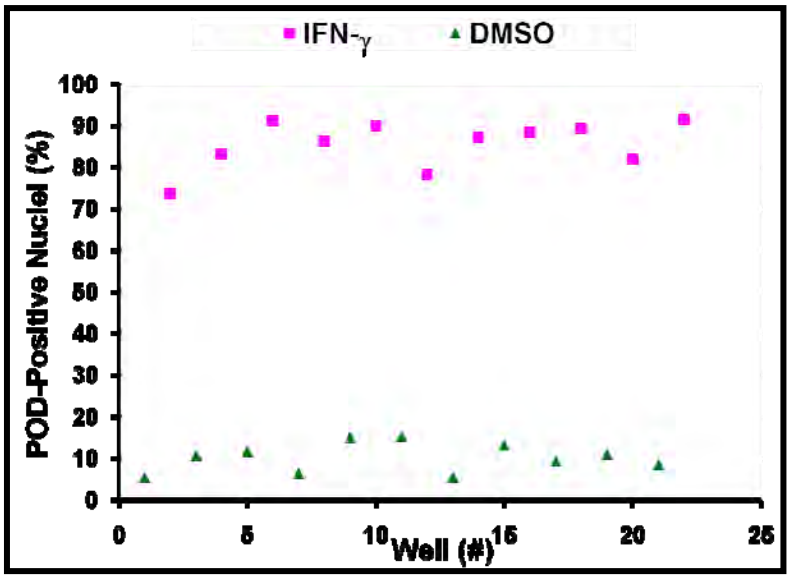

Figure 5. ***POD localization preliminary assay reproducibility assessment.*** HeLa cells were cultured overnight in 384-well plates (3150 cells/well), treated (12 h) with IFN-γ (2 U/μL) or DMSO (0.1%) for 12 h, immunostained for PML, imaged, and analyzed (n=11 wells/condition). The Z'-factor is 0.63.

Fluorophore-labeled anti-PML antibodies are available (which would eliminate the need for a secondary antibody and one set of washes), but its low fluorescent intensity made it impractical for high content screening (an integration time of over 1 s/image was required). In any case, our current primary assay procedure is high-throughput ready, and reproducible at a cost of 0.0923 cents/well, which is highly efficient for a HCS assay.

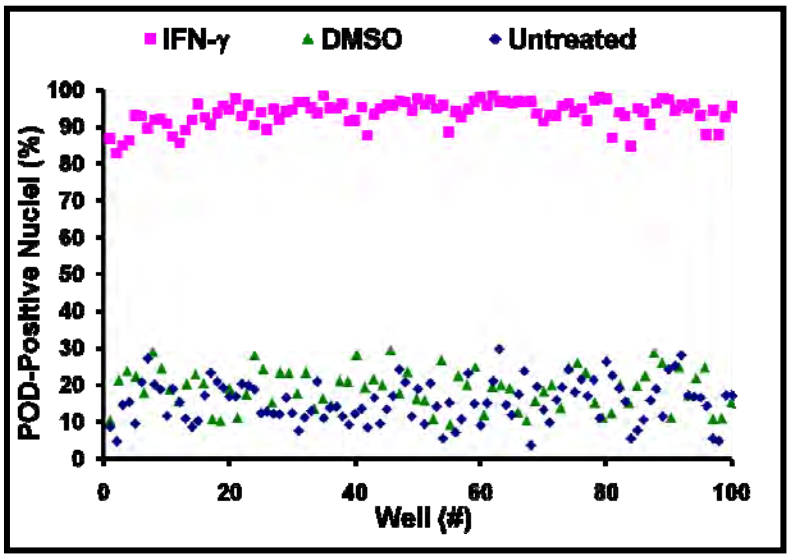

Figure 6. ***POD localization assay reproducibility assessment.*** HeLa cells were cultured overnight in 384-well plates (3150 cells/well), treated (12 h) with IFN-γ (2 U/μL), DMSO (0.1%), or nothing for 12 h, immunostained for PML, imaged, and analyzed (n=100 wells/condition). The Z'-factor is 0.64 or 0.65 using DMSO or untreated cells, respectively, as a negative control.

A manuscript was publication describing the development of the HCS assay (13).

Task #2. Screen chemical libraries to identify compounds that induce Daxx recruitment into PODs.

To further validate our assay, we conducted a preliminary screen of the Sigma-Aldrich LOPAC1280 chemical library (1280 compounds) and a combinatorial library provided by the Torrey Pines Institute for Molecular Studies (TPIMS). An example of primary data from the LOPAC1280 chemical screen (~5 µM final concentration) is provided in Figure 7. Compounds that increased the number of POD-positive nuclei by at least 50% (relative to the positive controls), as measured by the POD detection algorithm, were considered "hits". No hits were identified among LOPAC1280 compounds when screened at 5 µM. Moreover, dose-response curves (1:1 serial dilutions performed from 250 µM to 0.25 µM) were generated for the five LOPAC1280 compounds inducing the most POD-positivity, and the highest value observed was less than 40% POD-positive nuclei. These data suggest that the assay is highly specific and will not suffer from promiscuous reactivity with NIH library compounds.

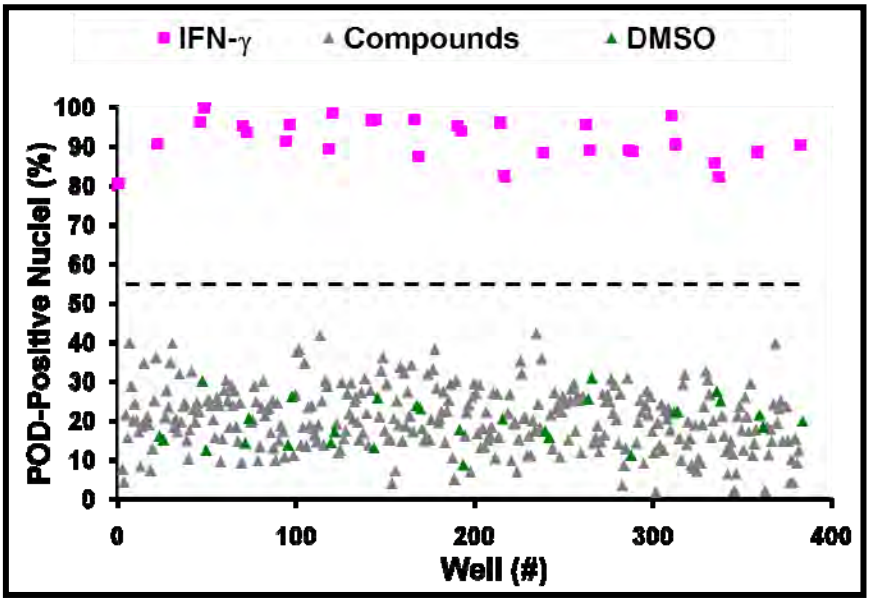

Figure 7. ***Sample plate from the LOPAC1280 POD localization screen.*** HeLa cells were seeded in 384-well plates (3150 cells/well) using the ThermoScientific Matrix WellMate and incubated at 37°C overnight. The cells were then treated for 12 h with DMSO (0.1%; negative control), IFN-γ (2 U/µL; positive control), or LOPAC1280 compounds. Plates were immunostained for PML, imaged, and analyzed. The Z'-factor was 0.55. (The dotted line represents the average value between positive and negative controls).

Next we screened mixture-based combinatorial libraries. The combinatorial library is formatted into 38 mixtures (dissolved in DMF), grouped according to scaffold, and represents 5,287,896 compounds (and several million peptides). Each mixture is present in two different wells at two different concentrations. This "scaffold ranking library" is used to determine the most active chemical scaffolds before further screening/deconvolution of mixtures. This library was screened at 5 µg/mL (~10 µM for average MW≈500 g/mol) and 10 µg/mL (~20 µM for average MW≈500 g/mol), with a Z'-factor of 0.6. The scaffold "1422" was the most active mixture (Figure 8). Screening of single discrete compounds belonging to this scaffold identified 8 "hit" compounds, each inducing POD-positive nuclei percentages above the average value between the positive and negative controls (Figure 9). Dose-response curves and POD-localization experiments in secondary cell lines have since confirmed these hits (*data not shown*).

When tested at 4 µg/mL (~8 µM for MW≈500 g/mol), 8 compounds induced POD formation in >50% of the cells, without cytotoxicity (Figure 9). At 10 µg/mL (~20 µM for MW≈500 g/mol), 50% of all 1422 compounds were toxic (data not shown). Thus, we recommend future screening at 5-8 µM.

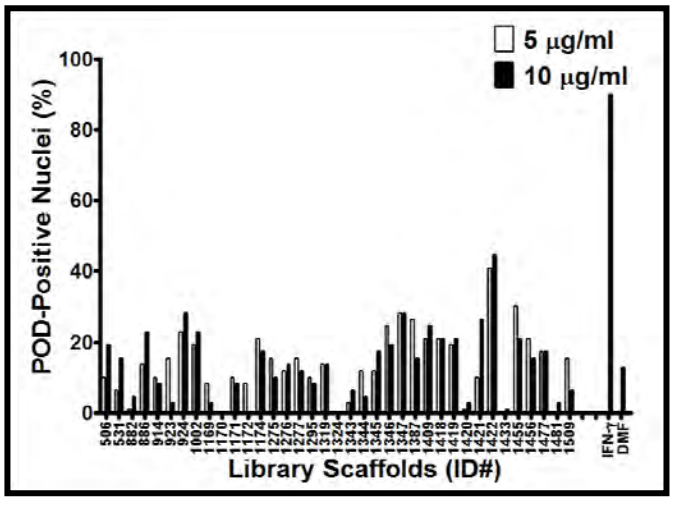

Figure 8. ***TPIMS Combinatorial Library POD localization screen.*** HeLa cells were seeded in 384-well plates (3150 cells/well) using the ThermoScientific Matrix WellMate and incubated at 37°C overnight. The cells were then treated for 12 h with DMF (0.1%; negative control), IFN-γ (2 U/µL; positive control), or mixtures from the TPIMS scaffold ranking library (5 µg/mL or 10 µg/mL, representing 10 µM or 20 µM, respectively, for MW≈500g/mol). Plates were immunostained for PML, imaged, and analyzed. The Z'-factor was 0.6.

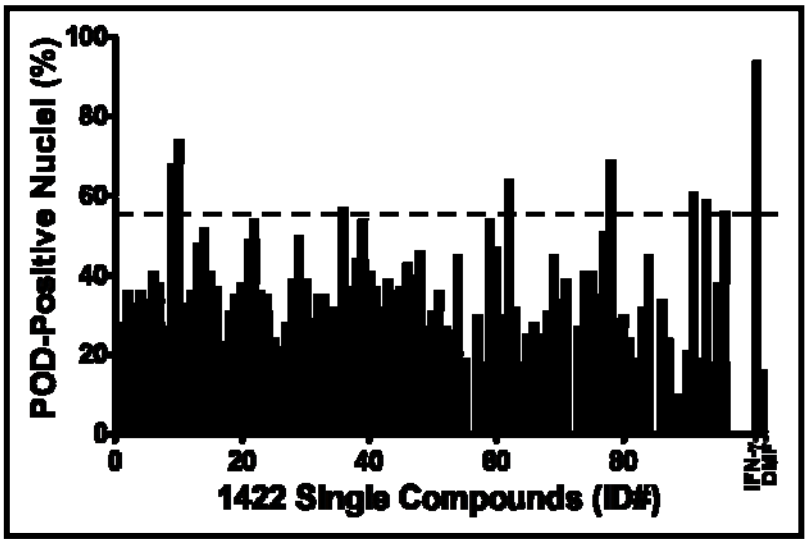

Figure 9. ***TPIMS 1422 Scaffold POD localization screen.*** HeLa cells were seeded in 384-well plates (3150 cells/well) using the ThermoScientific Matrix WellMate and incubated at 37°C overnight. The cells were treated for 12 h with DMF (0.1%; negative control), IFN-γ (2 U/µL; positive control), or single compounds from the TPIMS 1422 scaffold library (4 µg/mL, representing 8 µM for MW≈500 g/mol). Plates were immunostained for PML, imaged, and analyzed. The Z'-factor was 0.6. The dotted line represents the average value between positive and negative controls.

The work flow established for chemical library screening the HCS assay is depicted in Figure 10. The protocol details have been deposited into PubCHem.

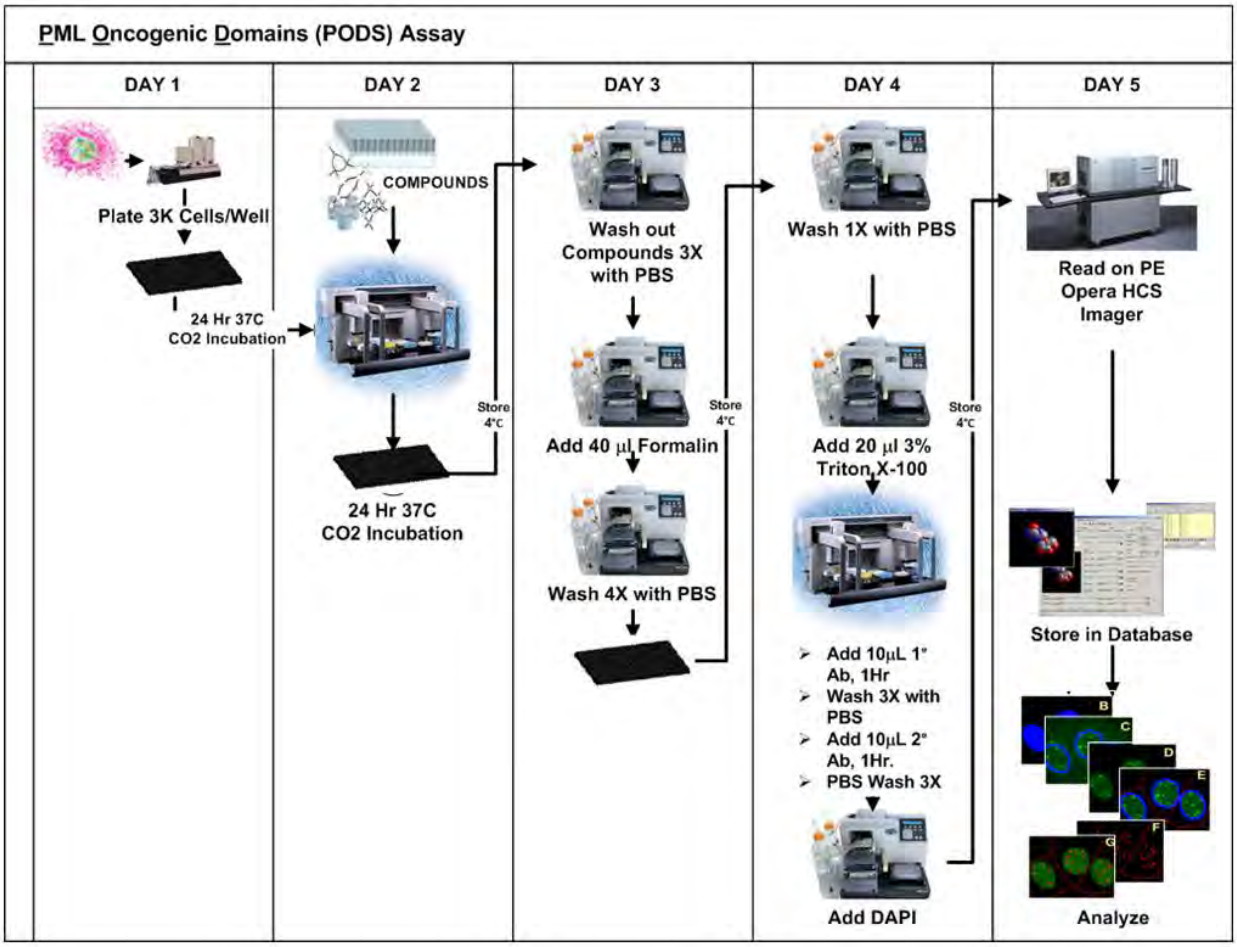

Figure 10. ***POD Activators Screen.*** Work-flow for POD activators screen is illustrated.

We then screened a large library of diverse chemicals with drug-like features (Sanford-Burnham's library). Altogether, 321,600 compounds were screened at an average concentration of 10 uM, from which 447 POD activators were identified. Additionally, 423 compounds were cytotoxic against the HeLa cells. These compounds were retested at a lower concentration (1 uM), revealing two more that induced PODs. All 76 POD activator were confirmed upon repeat testing. Of these 76, we were able to repurchase dry powder compounds for 58 and performed LC-MS analysis to verify their integrity, purity, and identity (Figure 11). Dose response analysis was performed for these 58 compounds, revealing 5 that induced PODs in a dose-dependent manner. Of these 5 promising hits, all passed a counter-screen that we developed using nuclear localization of histone γ-H2AX (see Task #4 below).

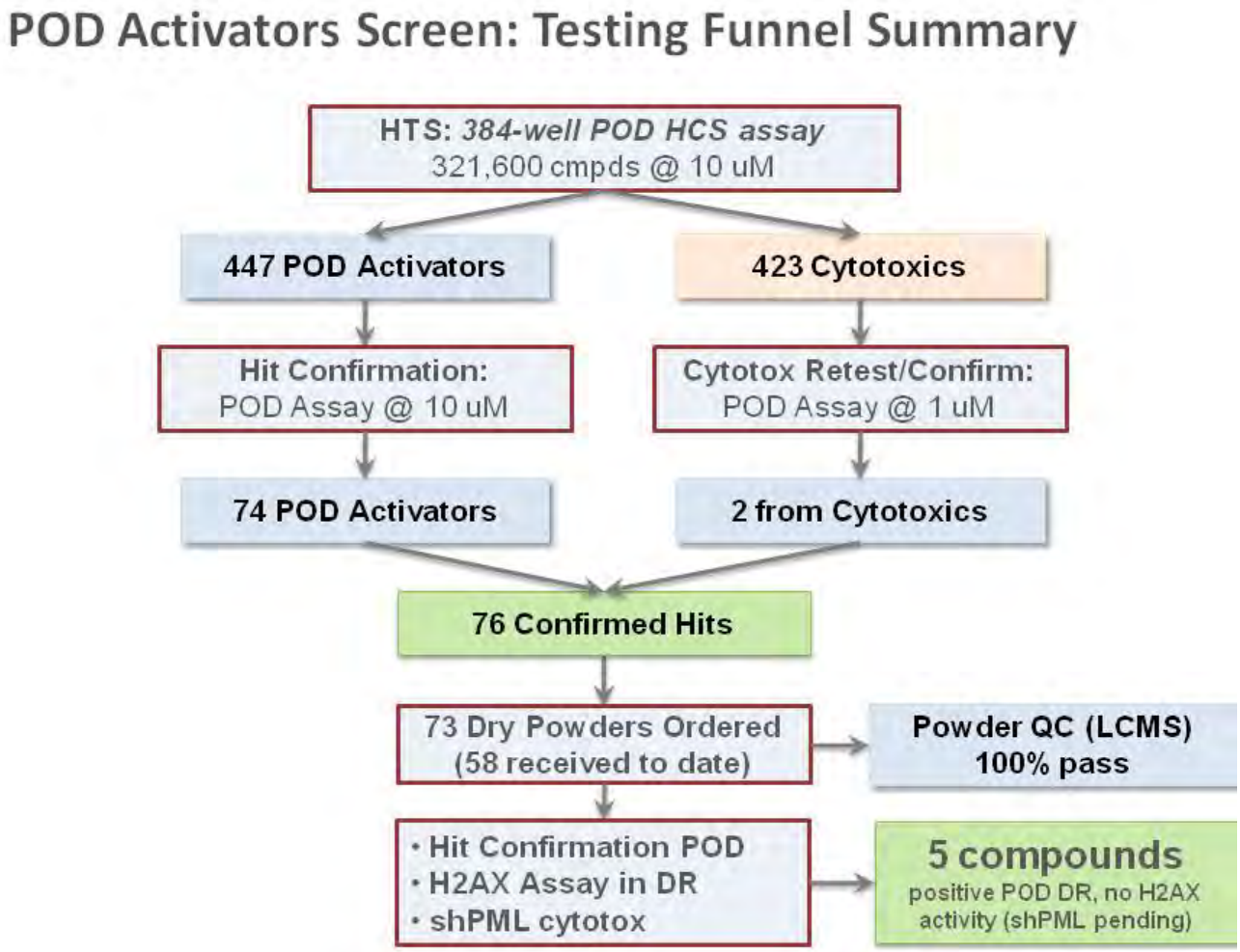

Figure 11. ***Chemical library screen for POD activators.*** The HCS assay was used in 384 well mode to screen a large library of drug-like compounds. See text above for details.

Task #3. Perform SAR studies on hits, revealing the structural features of compounds that drive activity.

Preliminary SAR on the TPIMS 1422 scaffold (N-methyl triamine) was derived from the combinatorial library deconvolution (Figure 12). TPIMS 1422 compounds were grouped into different mixtures (~1000 compounds/mixture), with each mixture containing compounds with similar R1, R2, or R3 groups. Screening of these mixtures yielded preliminary SAR information, and was used to synthesize the three most active TPIMS compounds to date (Figure 13).

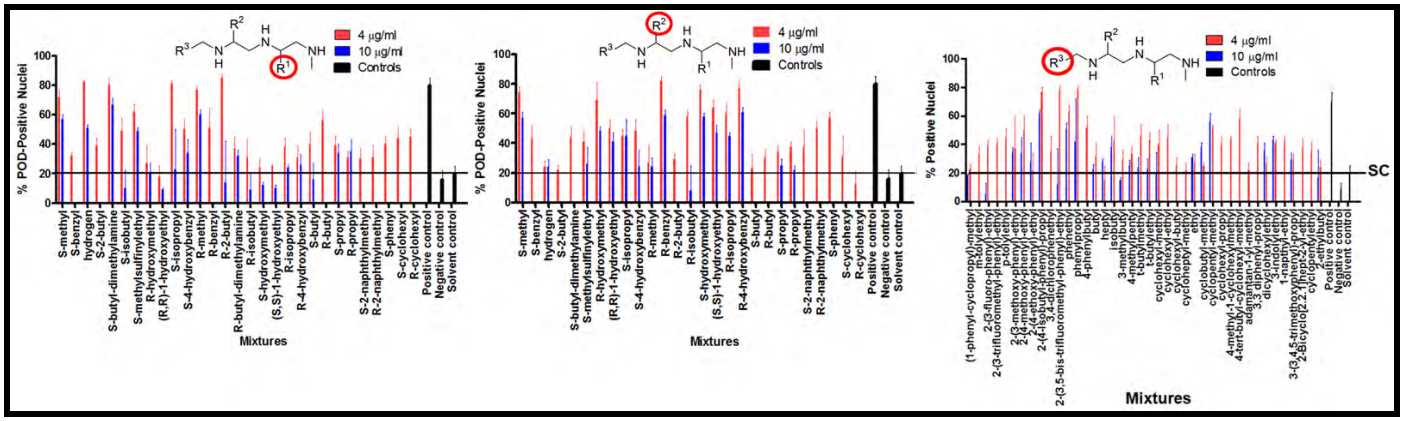

Figure 12. ***Preliminary TPIMS 1422 SAR studies.*** HeLa cells were seeded in 384-well plates (3150 cells/well) and incubated at 37°C overnight. The cells were then treated for 12 h with DMF (0.1%; negative control), IFN-γ (2 U/µL; positive control), or compound mixtures from the TPIMS 1422 scaffold library (4 µg/mL and 10 µg/mL representing 8 µM and 20 µM, respectively, for MW=500 g/mol). Each mixture contains (~1000 compounds/mixture) compounds with the indicated R1 (*left*), R2 (*center*), or R3 (*right*) groups. Plates were immunostained for PML, imaged, and analyzed. The solid line represents the solvent control value.

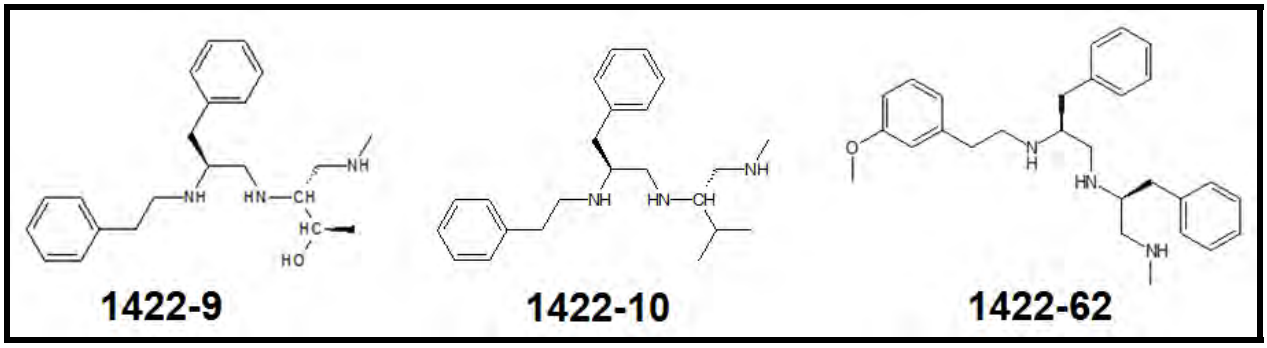

Figure 13. ***Structures of the most active TPIMS 1422 compounds.*** These compounds induce >90% POD-positive nuclei in HeLa cells, and are active against PPC-1 (hormone refractory prostate cancer) cells.

The combinatorial library contained groups of compounds with scaffolds that were chemically similar to the N-methyl triamines: TPIMS 1418 (N-methyl-1,4,5-trisubstituted-2,3-diketopiperazine), 1419 (N-benzyl-1,4,5-trisubstited-2,3-diketopiperazine), 1420 (N-methylated 1,3,4-trisubstituted piperazine), and 1421 (N-benzylated 1,3,4-trisubstituted piperazine). Mixtures of these compounds (grouped according to scaffold and R1 functional group) were assayed in a preliminary study of TPIMS 1422-related scaffolds (Figure 14). We anticipate that such a strategy will reveal numerous active TPIMS 1422-related discrete compounds.

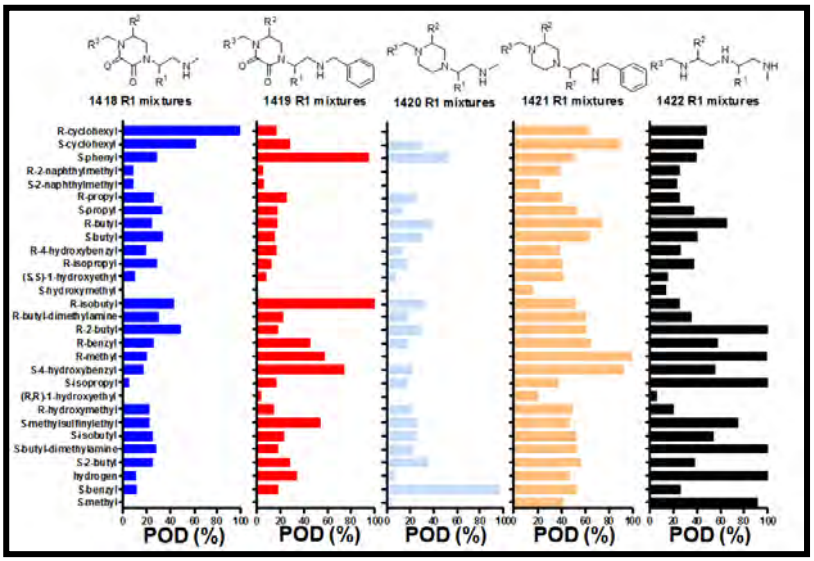

Figure 14. ***Preliminary study of TPIMS 1422-related scaffolds.*** HeLa cells were seeded in 384-well plates (3150 cells/well) and incubated at 37°C overnight. The cells were then treated for 12 h with DMF (0.1%; negative control), IFN-γ (2 U/µL; positive control), or compound mixtures (containing TPIMS 1422-related scaffolds (*top*); 4 µg/mL representing 8 µM for MW=500 g/mol). The R1 groups are indicated on the y-axis. Plates were immunostained for PML, imaged, and analyzed.

SAR analysis of hits from the screen of a large library of diverse compounds will be initiated if they pass the next phases of evaluation per the flow-chart in Figure 11.

Task #4. Test active compounds for pro-apoptotic activity against cultured PCa cell lines.

We generated PML stably knock-down HeLa cells for assessing the cytotoxic mechanism of POD activators. To this end, HeLa cells were stably transduced with recombinant retroviral vectors encoding PML shRNA versus scrambled control. Immunoblot analysis confirmed successful knock-down of the PML protein.

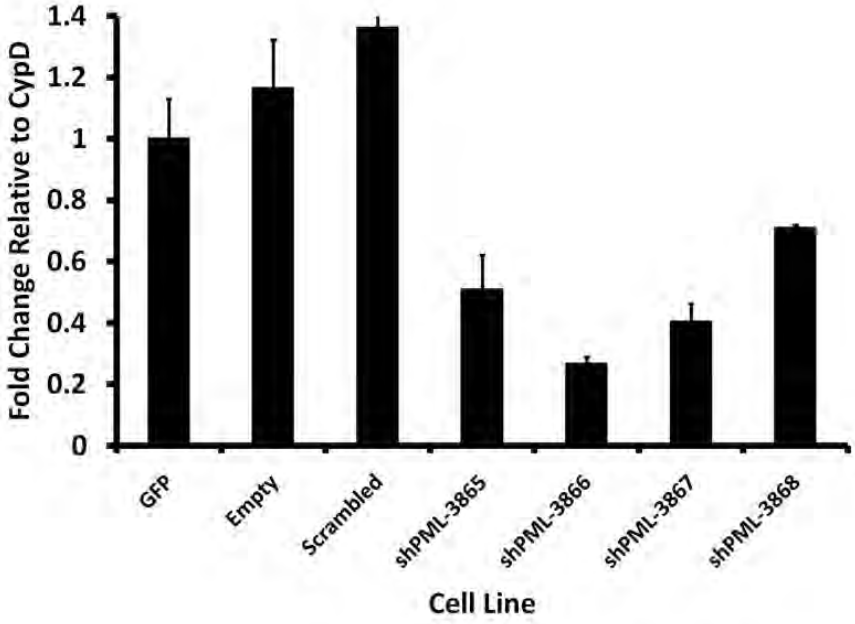

Figure 15. ***Q-RT-PCR of HeLa-shPML Stable Cell Lines.*** Four different shPML lentiviral vectors were generated (3865, 3966, 3867, and 3868), along with controls (GFP, empty, scrambled), and used to produce stably transfected HeLa cell lines. Cell lines were selected using puromycin (1-4 µg/mL). RNA was extracted and Q-RT-PCR was performed for PML mRNA and control CypD mRNA, expressing data as a ratio (mean ± std dev; n = 3).

Because arsenic trioxide induces apoptosis at least in part through a mechanism involving covalent modification of PML (14), we compared the cytotoxic responses of PML knockdown and control HeLa cells to AsO3. PML knockdown HeLa cells are relatively more resistant to AsO3-induced cytotoxicity (Figure 16).

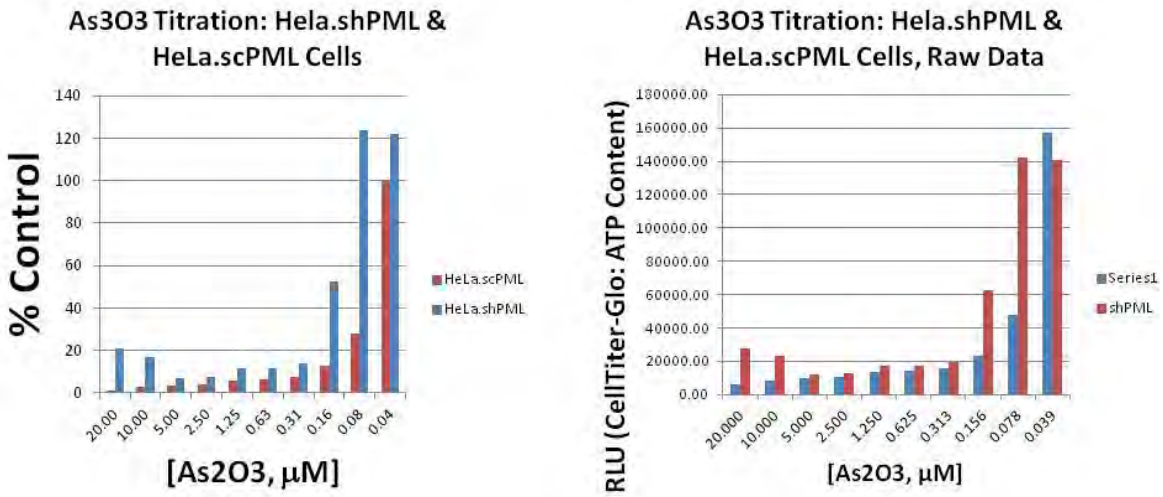

Figure 16. ***PML knockdown causes resistance to AsO3.*** HeLa cells with stably integrated scrambled control shRNA (blue) or PML shRNA (red) were cultured for 48 hrs with various concentrations of AsO3. Viable cell numbers were estimated by measuring cellular ATP levels using Cell Titer Glow (Promega). (Left) Data are expressed as % relative to

control untreated cells. (Right) Raw data are presented for Cell Titer Glow assay. Results represent mean ± std dev, n=3.

Because Interferon also induced apoptosis of HeLa cells via a PML-dependent mechanism, we compared PML knockdown and control cells with respect to sensitivity to Interferon-induced cytotoxicity. For these experiments, cells were cultured for various durations of time (0-4 days) with various concentrations of Interferon-g. The best results were obtained with 10-20 Units Interferon-g for 72 hrs, showing that PML is required for Interferon-g to kill HeLa cells (Figure 17).

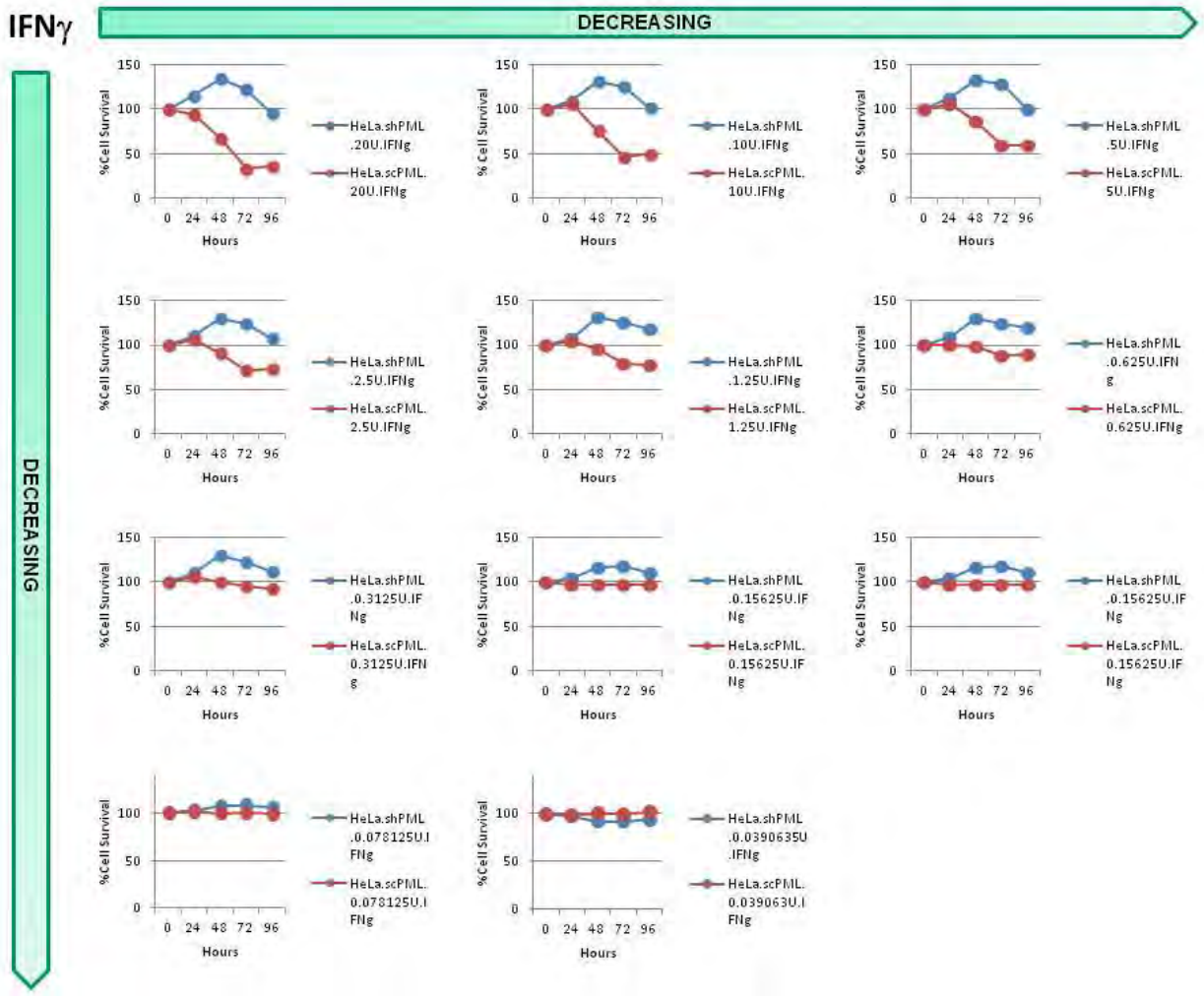

Figure 17. *Effects of IFNg on HeLa.shPML and HeLa.scPML Cells*. HeLa cell lines silenced (Hela.shRNA) for PML expression by shRNA (blue) and the control cell (HeLa.scPML) expressing scrambled shRNA (red) were exposed to decreasing concentrations of IFNg (20 U/ml declining 2X over 10 points) for 24-96 hours as indicated. Conditions: 3K cells/well in 384 well format with DMEM, FBS media at a 50 ul volume /test (n=16).

Standard colorimetric cell viability assays are suitable for initial screening but insufficient to characterize the mechanism of growth suppression (cytotoxic *vs* anti-proliferative). To create a robust automated platform for quantifying apoptosis for assessing impact of compounds in microwell format, we have used high-throughput microscopy (HTM). For this analysis, cells in 96 or 384 well plates are stained with DNA-binding fluorochrome DAPI, then the percentage of cells with apoptotic nuclear morphology is determined using algorithms previously developed by Dr. Price and colleagues using the Q3DM-Beckman Coulter IC 100 instrument in the Sanford-Burnham Center for Chemical Genomics (Figure 18).

Figure 18. ***Automated high-content analysis of apoptosis.*** Screen captures of representative histograms of DNA content with corresponding image fields (20X 0.5 N.A.) and cell montages representing apoptotic cells with sub G0 DNA content and high chromatin condensation (*top, right*) and metaphases/anaphases with G2 DNA content and high chromatin condensation (*lower, right*) are shown (15).

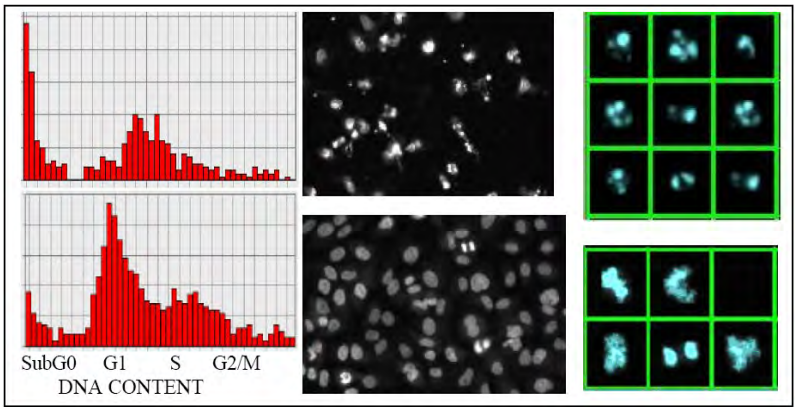

In preparation for testing PML/Daxx-activating compounds on prostate cancer cells, we genetically validated the importance of Daxx in these cells. To this end, we first generated a Daxx knock-down stable cell prostate cancer (PC) cell line. We started by comparing the endogenous Daxx levels among four human prostate cancer (PCa) cell lines (PC-3, ALVA-31, LNCaP, and DU145), so as to determine the most appropriate cell line for Daxx knock-down (Figure 19A). ALVA-31 was chosen for Daxx knock down studies, because of its higher endogenous levels of this protein. ALVA-31 is a hormone-refractory prostate cancer cell line. By employing a retroviral-mediated short hairpin (sh) RNA approach, we achieved ~ 90% Daxx knock-down efficiency compared to control shRNA-infected cells (Figure 19B). Daxx knock-down was quantified via reverse transcriptase-polymerase chain reaction (RT-PCR) for mRNA, and by protein immunobloting analyses (Figure 16B). Strikingly, when we compared Daxx levels in PCa cell lines to a nontumorigenic human prostatic epithelial line, PWR-1E, they were increased in all PCa lines examined (Figure 19C). Therefore, we have generated a stable Daxx knock-down PCa cell line, which mimics the normal prostate epithelial cells in Daxx protein levels.

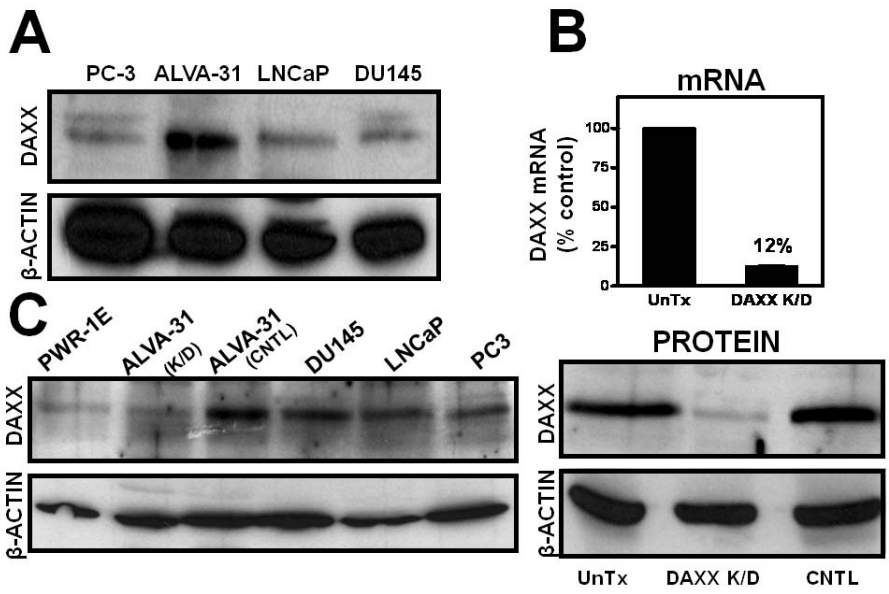

Figure 19. ***Silencing of Daxx in prostate cancer cell line ALVA-31.*** **(A)** Comparison of endogenous levels of Daxx among four prostate cancer (PCa) cell lines, PC-3, ALVA-31, LNCaP, and DU145. ALVA-31 cell line was chosen to knock down Daxx, because higher endogenous Daxx levels would facilitate subsequent phenotypic differences between wild type and Daxx knock-down cells. **(B)** Retroviral-mediated shRNA was used to stably silence Daxx in the hormone-refractory prostate cancer cell line ALVA-31. Daxx knock-down was quantified via reverse transcriptase-polymerase chain reaction (RT-PCR) for mRNA (top panel) and by immunobloting analyses for protein (bottom panel), revealing 88% knock-down efficiency (at the mRNA level) compared to control shRNA-infected cells. **(C)** Comparison of Daxx protein levels among various prostate cell lines. Lysates from six different cell types (PWR-1E, ALVA-31 Daxx K/D, ALVA-31 WT, DU145, LNCaP, and PC3) were normalized for total protein content (60 µg) and analyzed by SDS-PAGE and immunoblotting using antibodies specific for human Daxx and β-Actin. With the exception of PWR-1E, which is a nontumorigenic human prostatic epithelial line, all the other cell lines represent PCa lines. Daxx levels in normal prostate (PWR-1E) are low, and comparable to Daxx K/D ALVA-31 PCa line. Daxx levels increase in PCa cell lines.

We previously showed the Daxx regulates the expression of several apoptosis-regulating RelB target genes in mouse fibroblasts (16). We therefore tested the effects of Daxx gene knock-down on expression of some of these same genes in prostate cancer cells. Analysis of expression of RelB target genes by RT-PCR showed increased levels in Daxx-deficient compared to control ALVA31 cells of mRNAs encoding both the pro-apoptotic protein Dapk1 and anti-apoptotic proteins Bcl-B, c-Flip, and Birc3 (Figure 20A), thus phenocopying the effects of *daxx* gene ablation in mouse cells. These finding were confirmed at the protein level by immunoblotting (Figure 20B).

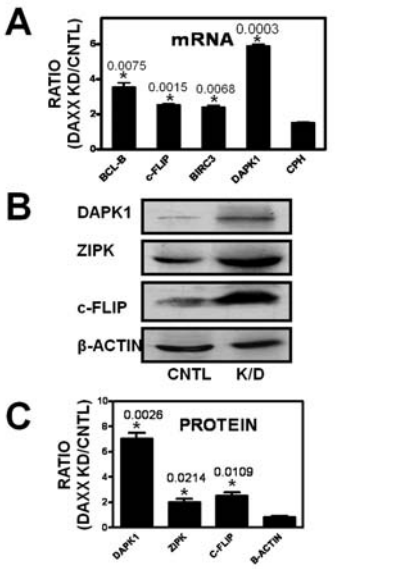

Figure 20. ***Reducing Daxx causes derepression of RelB target genes in ALVA-31 cells.*** Analysis of expression of RelB target genes by RT-PCR **(A)** showed increased levels in Daxx-deficient (K/D) compared to control ALVA31 (+/+) cells of mRNAs encoding pro-apoptotic protein Dapk1 (6 fold increase; p = 0.0003) and anti-apoptotic proteins Bcl-B (3.6 fold; p = 0.0075), c-Flip (2.6 fold; p = 0.0015), and Birc3 (cIAP2) (2.4 fold; p = 0.0068). These finding were confirmed at the protein level by immunoblotting **(B)**. **'*'** indicates the 'p' value relative to CPH (**A**) or β-Actin (**B**), and is < 0.05 for all genes examined.

In mouse fibroblasts, we should that ablation of the gene encoding Daxx results in reduced methylation of RelB target genes that regulate apoptosis (16). DNA methylation analyses using two different methods (affinity capture of methylated DNA (Figure 18A) and bisulfite sequencing (Figure18B)) demonstrated that Daxx controls epigenetic silencing of RelB target genes by DNA methylation also in prostate cancer cells. Specifically, the methylation of DAPK1 and c-FLIP target promoters was decreased in Daxx-deficient ALVA31 prostate cancer cells compared to control cells, while the methylation of TRAF6 control promoter remained unchanged (Figure 21). These results extend to prostate cancer cells our previous findings that Daxx regulates expression of apoptosis-relevant RelB target genes via DNA methylation (16)

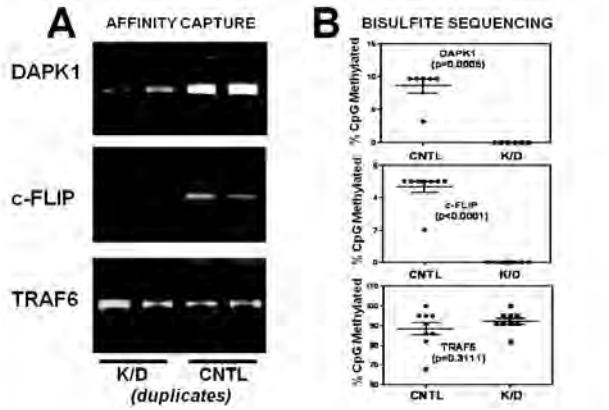

Figure 21. Reducing Daxx reduces methylation of RelB target genes in ALVA-31 cells. Genomic DNA was isolated from control (empty vector, Daxx +/+) or Daxx knock-down (K/D) ALVA-31 cells. DNA methylation analyses using two different methods (affinity capture **(A)** or bisulfite sequencing **(B)**) demonstrated that Daxx controls DNA methylation of RelB target genes.

<u>Counter-Screen for DNA Damaging Agents</u>. DNA damaging agents can induce POD formation in some types of cells, but our goal is to avoid such agents as candidates for further development. Thus, we devised a secondary counter-screening assay to eliminate such compounds from further consideration. DNA damage is primarily "sensed" by the kinases ATM and ATR, which sense double-stranded DNA breaks and single-stranded DNA breaks (a common intermediate found at sites of DNA damage detection and repair pathways; e.g. nucleotide excision repair, homologous recombination repair, and DNA damage-induced stalled replication forks), respectively (17). H2AX is phosphorylated primarily by ATM (also by ATR under some circumstances), while Chk1 is phosphorylated primarily by ATR (also by ATM under some circumstances) (17).

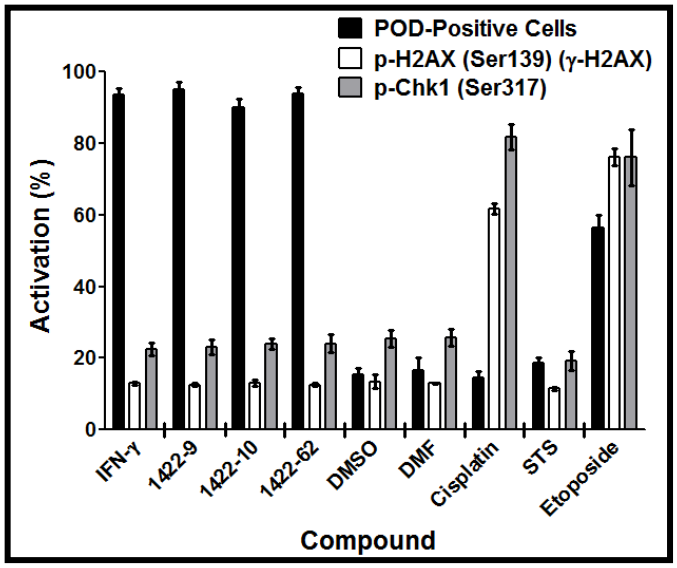

Figure 22. ***Detecting DNA damage and POD formation.*** HeLa cells were seeded in 384-well plates (3150 cells/well) using the ThermoScientific Matrix WellMate and incubated at 37°C overnight. The cells were treated for 12 h with IFN-γ (2 U/μL), 1422 compounds (4 μg/mL representing 8 μM for MW=500 g/mol), DMSO (0.1%), DMF (0.1%), cisplatin (25 μM), staurosporine (25 nM), or etoposide (25 μM). Plates were then immunostained for PODs (mouse monoclonal anti-PML, Alexa Fluor 488 chicken anti-mouse antibodies), phospho-H2AX (rabbit polyclonal anti-phospho-H2AX-Ser139, Alexa Fluor 568 goat anti-rabbit antibodies), or phospho-Chk1 (rabbit polyclonal anti-phospho-Chk1-Ser317, Alexa Fluor 568 goat anti-rabbit antibodies). POD positive nuclei (%) were quantified as previously described. p-H2AX and p-Chk1 nuclear staining intensity was quantified using CytoShop. Mean and standard deviation are shown (n=4 wells/condition).

Phospho-H2AX (Ser139) (γ-H2AX) and phospho-Chk1 (Ser317) immunofluorescence staining, quantified using CytoShop algorithms, can be used as a preliminary counter-screen to detect compounds that induce DNA damage (Figure 22). For phospho-H2AX and phospho-Chk1, polyclonal rabbit antibodies were used, possibly allowing one of these antibodies to be used during the POD dose-responses (which uses a monoclonal mouse antibody) to multiplex the assay to detect both POD induction and DNA damage. A non-interfering secondary antibody would be used (such as in Figure 22).

From Figure 22, it can be seen that IFN-γ (POD-positive control) increased POD-positivity and did not increase phospho-H2AX or phospho-Chk1 staining beyond solvent controls (negative controls). Cisplatin (DNA damage control) did not increase POD-positivity, but increased phospho-H2AX and phospho-Chk1 positivity as expected. Staurosporine (cell death control) did not increase POD or DNA damage positivity. Etoposide, known to induce PODs and DNA damage (18), increased POD-, phospho-H2AX-, and phospho-Chk1-positivity, as expected (19, 20). Finally, the three most active TPIMS 1422 compounds (9, 10, and 62) did not induce DNA damage.

Task #5. Optimize potency and selectivity of active compounds by medicinal chemistry for Daxx recruitment to PODs.

This Task has not yet been initiated, beyond deconvolution of the combinatorial libraries. When further hit compounds have been validated, then we will generate our optimization strategies and proceed.

Task #6. Assess in vivo pharmacology and toxicology of active compounds.

This Task has not yet been initiated. When compound optimization begins, we will integrate assessments of pharmaceutical properties into the optimization strategy.

Task #7. Test active compounds for anti-tumor activity using PCa xenografts in mice.

Compounds are not yet ready for testing in vivo. However, in the past year, we established both subcutaneous and orthotopic prostate cancer tumor xenograft models in mice and thus will be poised to undertake the studies when the project progresses to this point.

KEY RESEARCH ACCOMPLISHMENTS

1. Developed HCS assay for compound library screening and validated POD assay with pilot library screen.

2. Developed secondary counter-screening assay to eliminate compounds that induce DNA damage.

3. Identified POD-activating compounds from mixture-based combinatorial chemical libraries.

4. Identified POD-activating compounds from traditional synthetic compound library.

5. Validated cellular PML-dependent cytotoxicity assays using AsO3 and Interferon-g.

6. Genetically verified that Daxx functions as a repressor of apoptosis-regulating RelB target genes in hormone refractory prostate cancer cells.

7. Prepared stable PML and Daxx shRNA-mediated knock down PCa cells for evaluation of the mechanism of POD activating compounds that display cytotoxic activity.

REPORTABLE OUTCOMES

1. HCS assay protocol established and published.

2. First-generation POD-activating compounds identified from both combinatorial libraries and diverse chemical libraries.

3. Stable PML and Daxx knock-down HeLa cells and in ALVA31 prostate cancer cell lines established and characterized, proving tools for mechanism of action (MOA) analysis of hits.

REFERENCES

1. Salomoni P, Pandolfi PP. The role of PML in tumor suppression. Cell. 2002;108:165-70.
2. Takahashi Y, Lallemand-Breitenbach V, Zhu J, De The H. PML nuclear bodies and apoptosis. Oncogene. 2004 Apr 12;23(16):2819-24.
3. Wang ZG, Ruggero D, Ronchetti S, Zhong S, Gaboli M, Rivi R, et al. PML is essential for multiple apoptotic pathways. Nat Genet. 1998 Nov;20(3):266-72.
4. Everett RD, Freemont P, Saitoh H, Dasso M, Orr A, Kathoria M, et al. The disruption of ND10 during herpes simplex virus infection correlates with the Vmw110-and proteasome-dependant loss of several PML isoforms. J Virol. 1998;72:6581-91.
5. Kawai T, Akira S, Reed JC. ZIP kinase triggers apoptosis from nuclear PML oncogenic domains (PODs). Mol Cell Biol. 2003;23(17):6174-86.
6. Becker KA, Florin L, Sapp C, Maul GG, Sapp M. Nuclear localization but not PML protein is required for incorporation of the papillomavirus minor capsid protein L2 into virus-like particles. J Virol. 2004 Feb;78(3):1121-8.
7. Hofmann H, Sindre H, Stamminger T. Functional interaction between the pp71 protein of human cytomegalovirus and the PML-interacting protein human Daxx. J Virol. 2002 Jun;76(11):5769-83.
8. Bell P, Lieberman PM, Maul GG. Lytic but not latent replication of epstein-barr virus is associated with PML and induces sequential release of nuclear domain 10 proteins. J Virol. 2000 Dec;74(24):11800-10.
9. Doucas V, Ishov AM, Romo A, Juguilon H, Weitzman MD, Evans RM, et al. Adenovirus replication is coupled with the dynamic properties of the PML nuclear structure. Genes Dev. 1996 Jan 15;10(2):196-207.
10. Torii S, Egan DA, Evans RA, Reed JC. Human Daxx regulates Fas-induced apoptosis from nuclear PML oncogenic domains (PODs). Embo J. 1999 Nov 1;18(21):6037-49.
11. Croxton R, Puto LA, de Belle I, Thomas M, Torii S, Hanaii F, et al. Daxx represses expression of a subset of antiapoptotic genes regulated by nuclear factor-kappaB. Cancer Res. 2006;66:9026-35.
12. Marcelli M, Stenoien D, Szafran A, Simeoni S, Agoulnik I, Weigel N, et al. Quantifying Effects of Ligands on Androgen Receptor Nuclear Translocation, Intranuclear Dynamics, and Solubility. J of Cellular Biochemistry. 2006;98:770-8.
13. Yip KW, Cuddy M, Pinilla C, Giulanotti M, Heynen-Genel S, Matsuzawa S, et al. A High-Content Screening (HCS) Assay for the Identification of Chemical Inducers of PML Oncogenic Domains (PODs). J Biomol Screen. 2011 Feb;16(2):251-8.
14. Zhang XW, Yan XJ, Zhou ZR, Yang FF, Wu ZY, Sun HB, et al. Arsenic trioxide controls the fate of the PML-RARalpha oncoprotein by directly binding PML. Science. 2010 Apr 9;328(5975):240-3.
15. Coulter QD-B. Analysis of Proliferation and Apoptosis Using the IC/EIDAQ 100 High Throughput Microscopy System. Application Note provided with the IC 100 HCS instrument. 2004.
16. Puto LR, J.C. . Daxx represses RelB target promoters via DNA methyltransferase recruitment and DNA hypermethylation. Genes Dev. 2008 April 15;22(8):998-1010.
17. Sancar A, Lindsey-Boltz LA, Unsal-Kacmaz K, Linn S. Molecular mechanisms of mammalian DNA repair and the DNA damage checkpoints. Annu Rev Biochem. 2004;73:39-85.
18. Dellaire G, Ching RW, Ahmed K, Jalali F, Tse KC, Bristow RG, et al. Promyelocytic leukemia nuclear bodies behave as DNA damage sensors whose response to DNA double-strand breaks is regulated by NBS1 and the kinases ATM, Chk2, and ATR. J Cell Biol. 2006 Oct 9;175(1):55-66.

19. Tanaka T, Halicka HD, Traganos F, Seiter K, Darzynkiewicz Z. Induction of ATM activation, histone H2AX phosphorylation and apoptosis by etoposide: relation to cell cycle phase. Cell Cycle. 2007 Feb;6(3):371-6.
20. Montecucco A, Biamonti G. Cellular response to etoposide treatment. Cancer Lett. 2007 Jul 8;252(1):9-18.

A High-Content Screening (HCS) Assay for the Identification of Chemical Inducers of PML Oncogenic Domains (PODs)

KENNETH W. YIP,[1,*] MICHAEL CUDDY,[1] CLEMENCIA PINILLA,[2] MARC GIULANOTTI,[3] SUSANNE HEYNEN-GENEL,[4] SHU-ICHI MATSUZAWA,[1] and JOHN C. REED[1,4]

PML is a multi-functional protein with roles in tumor suppression and host defense against viruses. When active, PML localizes to subnuclear structures named PML oncogenic domains (PODs) or PML nuclear bodies (PML-NBs), whereas inactive PML is located diffusely throughout the nucleus of cells. The objective of the current study was to develop a high content screening (HCS) assay for the identification of chemical activators of PML. We describe methods for automated analysis of POD formation using high throughput microscopy (HTM) to localize PML immunofluorescence in conjunction with image analysis software for POD quantification. Using this HCS assay in 384 well format, we performed pilot screens of a small synthetic chemical library and mixture-based combinatorial libraries, demonstrating the robust performance of the assay. HCS counter-screening assays were also developed for hit characterization, based on immunofluorescence analyses of the subcellular location of phosphorylated H2AX or phosphorylated CHK1, which increase in a punctate nuclear pattern in response to DNA damage. Thus, the HCS assay devised here represents a high throughput screen that can be utilized to discover POD-inducing compounds that may restore the tumor suppressor activity of PML in cancers or possibly promote anti-viral states. (*Journal of Biomolecular Screening* 2011;16:251-258)

Key words: PML, POD, nuclear bodies, apoptosis, high content screening

INTRODUCTION

PROMYELOCYTIC LEUKEMIA PROTEIN (PML) ONCOGENIC DOMAINS (PODs), also known as PML nuclear bodies (PML-NBs), Kremer bodies, ND10 (nuclear domain 10), or nuclear dots (NDs), are ~0.2- to 1-µm subnuclear structures present in a wide variety of cell types.[1,2] PML is required for the formation of PODs, and more than 30 proteins either transiently or constitutively co-localize with PML in PODs.[2] The significance of the *PML* gene was first noted in acute promyelocytic leukemia (APL), wherein the vast majority of cases are characterized by t(15;17) chromosomal translocations that result in a PML-RARα fusion protein that disrupts PML function by delocalizing PML into microspeckled nuclear structures (the reciprocal RARα-PML fusion protein disrupts RARα function).[3] Expression of PML-RARα in the promyelocytic/myeloid compartment of transgenic mice causes leukemia with APL features, underscoring the tumor-suppressive activity of PODs.[1-3]

PML plays an essential role in both caspase-dependent and caspase-independent cell death.[2] *pml–/–* mice are resistant to apoptosis induced by numerous stimuli and have an increased tumor incidence.[4,5] PML contributes to cell death induced by γ-radiation, the primary treatment modality for a wide variety of tumors.[6] Interferons and arsenicals (e.g., As_2O_3) increase the number and size of PODs per cell and sensitize and/or induce apoptosis in a variety of tumor cell types.[7,8] Interestingly, PML confers direct resistance to many viruses, and numerous viruses have evolved mechanisms for disrupting POD formation.[9]

Among the proteins that localize to PODs are p53, Daxx, and RecQ DNA helicase. The tumor suppressor p53 requires acetylation by CBP/p300 at PODs for the induction of apoptosis.[2,10] Daxx localization to PODs increases PTEN nuclear localization and PTEN tumor suppressor activity by inhibiting

[1]Sanford-Burnham Medical Research Institute, La Jolla, CA, USA.
[2]Torrey Pines Institute for Molecular Studies, San Diego, CA, USA.
[3]Torrey Pines Institute for Molecular Studies, Port Saint-Lucie, FL, USA.
[4]Conrad Prebys Center for Chemical Genomics, Sanford-Burnham Medical Research Institute, La Jolla, CA, USA.
[*]Current address: University of Toronto, Toronto, Canada.

Received Aug 31, 2010, and in revised form Oct 19, 2010. Accepted for publication Oct 21, 2010.

Journal of Biomolecular Screening 16(2); 2011
DOI: 10.1177/1087057110394181

HAUSP-mediated PTEN deubiquitinylation.[11] PTEN nuclear exclusion is associated with cancer progression, and HAUSP overexpression coincides with PTEN nuclear exclusion in prostate cancer.[11] Daxx also represses the transcription of various antiapoptotic Rel-B-associated genes, including cIAP2, cFLIP, and Bfl-1 (A1), via histone deacetylase (HDAC) and DNA methyltransferase binding and recruitment.[12,13] PODs are required for the maintenance of genomic stability in combination with proteins such as RecQ DNA.[14] Notably, PML also suppresses the anchorage-independent growth of transformed cells, is required for hypophosphorylated Rb-mediated cell cycle arrest, and inhibits neoangiogenesis in human and mouse tumors.[1,15]

The fundamental roles of PODs and POD-related proteins in tumor suppression validate targeting PODs for drug discovery. POD formation is essential in interferon and arsenical cancer therapy, especially for leukemias and multiple myeloma.[2,16,17] Interferons and arsenicals, however, induce a plethora of toxic effects, limiting their effectiveness.[17,18] The objective of the current study was to develop a high-content screening (HCS) assay for the high-throughput identification of chemical activators of PODs.

MATERIALS AND METHODS

Cell culture

HeLa cells were originally obtained from ATCC (Manassas, VA) and cultured in Dulbecco's modified Eagle's medium (DMEM; Invitrogen, Carlsbad, CA), with 10% fetal bovine serum (FBS; Clontech, Mountain View, CA) and penicillin-streptomycin (diluted according to the manufacturer's specifications; Invitrogen) at 37 °C, 5% CO_2. PPC-1 cells were cultured similarly but with RPMI 1640 (Invitrogen) instead of DMEM.

Compounds

The LOPAC^{1280} collection of 1280 pharmacologically active single compounds was obtained from Sigma-Aldrich (St. Louis, MO). The Torrey Pines Institute for Molecular Studies Combinatorial Libraries are mixture-based libraries in positional scanning format, and they were dissolved in dimethylformamide (DMF).[19-21]

Immunofluorescence assay

In total, 3150 cells/well (50-µL/well volume) were seeded onto 384-well clear-bottom plates (Greiner Bio-One, Monroe, NC) using the Matrix WellMate liquid dispenser (Thermo Fisher Scientific, Hudson, NH) and incubated at 37 °C (5% CO_2). After 24 h, the Biomek FX Laboratory Automation Workstation (Beckman Coulter, Fullerton, CA) was used to add interferon-γ (IFN-γ; 4 U/µL with either 0.1% DMSO or DMF; R&D Systems, Minneapolis, MN), DMSO (0.1% final concentration; Sigma-Aldrich), DMF (0.1% final concentration; Sigma-Aldrich), or compounds. After 12 h, cells were washed with phosphate-buffered saline (PBS), fixed with 4% formaldehyde (Sigma-Aldrich) for 15 min, washed, permeabilized with 0.5% Triton X-100 (Sigma-Aldrich) for 5 min, washed, incubated with the primary antibody diluted to 0.5 µg/mL in 5% bovine serum albumin (BSA; Thermo Fisher Scientific) for 1 h, washed, incubated with the secondary antibody diluted to 5 µg/mL in 5% BSA for 1 h, washed, and placed in a 100-ng/mL DAPI-PBS solution (Invitrogen) overnight. Each wash step was a multiple fluid change using the Titertek MAP-C II Microplate Washer and Stacker (aspiration to 10 µL, 50 µL PBS addition, repeated a total of 3 times; Titertek, Huntsville, AL).

For PML immunostaining, mouse monoclonal antihuman PML primary antibody (PG-M3, Santa Cruz Biotechnology, Santa Cruz, CA) was used with an Alexa Fluor 488 chicken antimouse IgG secondary antibody (Invitrogen). For phospho-H2AX (Ser139; p-H2AX or γ-H2AX) or phospho-Chk1 (Ser317) immunostaining, rabbit polyclonal antihuman phosphohistone H2A.X (Ser139; diluted 1:400; Cell Signaling Technology, Danvers, MA) or phospho-Chk1 (Ser317; diluted 1:400; Cell Signaling Technology) primary antibodies were used, respectively, with an Alexa Fluor 568 goat antirabbit IgG secondary antibody (Invitrogen).

High-content imaging

Plates were imaged using the Beckman Coulter Cell Lab IC-100 Image Cytometer with a 40× 0.6NA ELWD Plan Fluor dry (air) objective (6 images/well). The images (>200 cells/well) were analyzed using the POD detection algorithm, which was developed based on CytoShop (Beckman Coulter) and MATLAB (MathWorks, Natick, MA) software.

HCS was performed at the Conrad Prebys Center for Chemical Genomics at the Sanford-Burnham Medical Research Institute (La Jolla, CA).

Statistical analyses

HCS performance was characterized using the following equation: $Z' \text{ factor} = 1 - (3\sigma_{positive} + 3\sigma_{negative})/|(\mu_{positive} - \mu_{negative})|$, where $\sigma_{positive}$ is the standard deviation of the positive control, $\sigma_{negative}$ is the standard deviation of the negative control, $\mu_{positive}$ is the mean of the positive control, and $\mu_{negative}$ is the mean of the negative control.[22]

RESULTS

Development and optimization of the PML-POD localization assay

Immunostaining conditions were optimized for detection of PML using a commercially available mouse monoclonal antibody. HeLa cells were seeded in 384-well plates, treated with either DMSO or IFN-γ for 24 h, and immunofluorescently

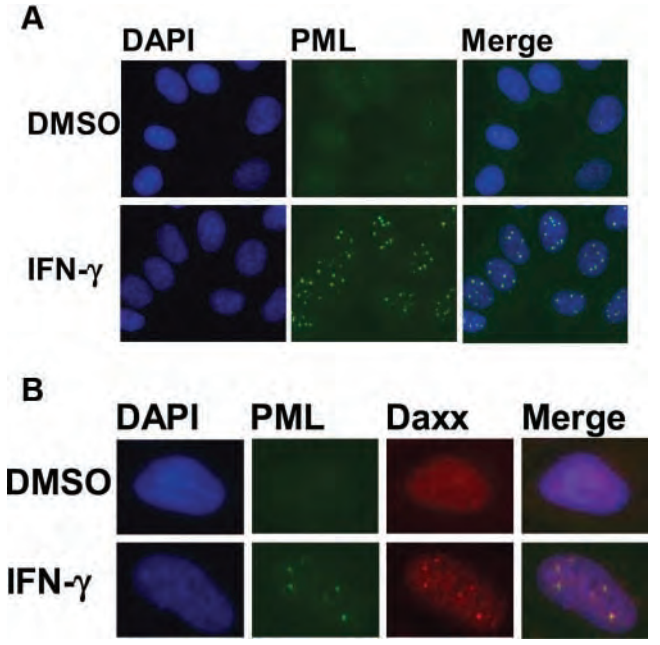

FIG. 1. PML and Daxx localize to PML oncogenic domains (PODs) after interferon-γ (IFN-γ) treatment. (**A**) PML localizes to nuclear bodies. HeLa cells were seeded in 384-well plates (3150 cells/well), treated (12 h) with DMSO (0.1%) or IFN-γ (4 U/μL), immunostained with mouse monoclonal antihuman PML and Alexa Fluor 488 chicken antimouse antibodies (green), and incubated in DAPI (nuclear stain; 100 ng/mL; blue). Cells were imaged using the Cell Lab IC-100 Image Cytometer (40× 0.6NA ELWD Plan Fluor objective). (**B**) PML and Daxx co-localize to PODs. Cells were treated and imaged as in **A** but also immunostained for Daxx (rabbit polyclonal antihuman Daxx primary antibody, Alexa Fluor 568 goat antirabbit secondary antibody; red).

stained for PML to confirm IFN-γ-induced PML localization into PODs (**Fig. 1A**). IFN-γ-induced localization of PML into PODs is accompanied by the localization of various other proteins to PODs, such as Daxx.[23] Thus, simultaneous immunofluorescence detection of both PML and Daxx in HeLa cells confirmed co-localization/formation of PODs and validated IFN-γ as a positive control (**Fig. 1B**). IFN-γ-induced PML and Daxx co-localization to PODs was also confirmed to occur in PPC-1 cells (observed by immunofluorescence; data not shown).

To quantify the extent of POD formation (i.e., the number of PODs per cell, the intensity of PML localization, and the fraction of cells per well with extensive numbers of PODs) in an automated fashion, the "POD detection algorithm" was developed using Beckman Coulter CytoShop and MathWorks MATLAB software (**Fig. 2A**). First, the nuclear image (DAPI stain) was used to produce a "nuclear mask," which identified all nuclei in an image. This nuclear mask was applied to the PML ("green") image, and all green pixels outside of this nuclear mask were eliminated. Next, PODs were outlined based on the identification of green pixels with higher intensities than their surrounding pixels (using CytoShop's "Aggregate Detection"), with the minimum size of a POD defined based on IFN-γ control wells (CytoShop's "Object Scale"). This number of detected PODs was then reported on a per nucleus basis and used to determine the percentage of nuclei per image that were "POD positive." The value for the number of detected PODs above which a nucleus is considered POD positive was determined to be 4.0 by iteratively setting increasing threshold values and determining the Z′ factor for each threshold (on control plates).

To both further validate the algorithm, HeLa cells were treated with increasing concentrations of IFN-γ, stained with anti-PML antibody, and imaged, and the percentage of POD-positive cells was determined (**Fig. 2B**). Using this automated method, IFN-γ was determined to induce concentration-dependent POD formation in HeLa cells. Manual counting of POD-positive cells confirmed the algorithm-defined quantification (data not shown). Examples of whole-field images from single wells (multiple images from single wells) are shown in Supplemental Figure S1 (**online at http://jbx.sagepub.com/content/by/supplemental-data**).

To characterize the reproducibility of the assay, multiple replicates were prepared ($n > 80$ per condition), where cells were seeded into a 384-well plate using the Matrix Wellmate bulk liquid dispenser (3150 cells/well); treated with IFN-γ (4 U/μL), DMSO (0.1%), or nothing for 12 h; and immunostained for PML, imaged, and analyzed. The Z′ factor was determined to be 0.64 or 0.65 using DMSO or untreated cells, respectively, as the negative control (**Fig. 2C**).

High-content screening

The HCS assay was used to screen the LOPAC^{1280} library of pharmacologically active compounds for PML activators (**Fig. 3A**). Compounds that increased the number of POD-positive nuclei by at least 50% (relative to the controls), as measured by the POD detection algorithm, were considered hits. No hits were identified when the library was screened at 5 μM. Moreover, dose-response curves (serial dilutions performed from 250 μM to 0.25 μM) were generated for the 5 LOPAC^{1280} compounds inducing the most POD positivity, and the highest value observed was less than 40% POD-positive nuclei (data not shown). Thus, the HCS assay is not promiscuous with respect to hit rate.

The TPIMS mixture-based combinatorial libraries were formatted and plated as a "scaffold ranking library," which was subsequently screened to determine the most active chemical scaffolds before further screening/deconvolution of mixtures.[24] The scaffold ranking library was formatted as 38 mixtures (dissolved in DMF), grouped according to scaffold, and represented 5,287,896 compounds (and several million peptides). Each mixture was present in 2 different wells at 2 different concentrations. Use of mixtures makes it readily feasible to

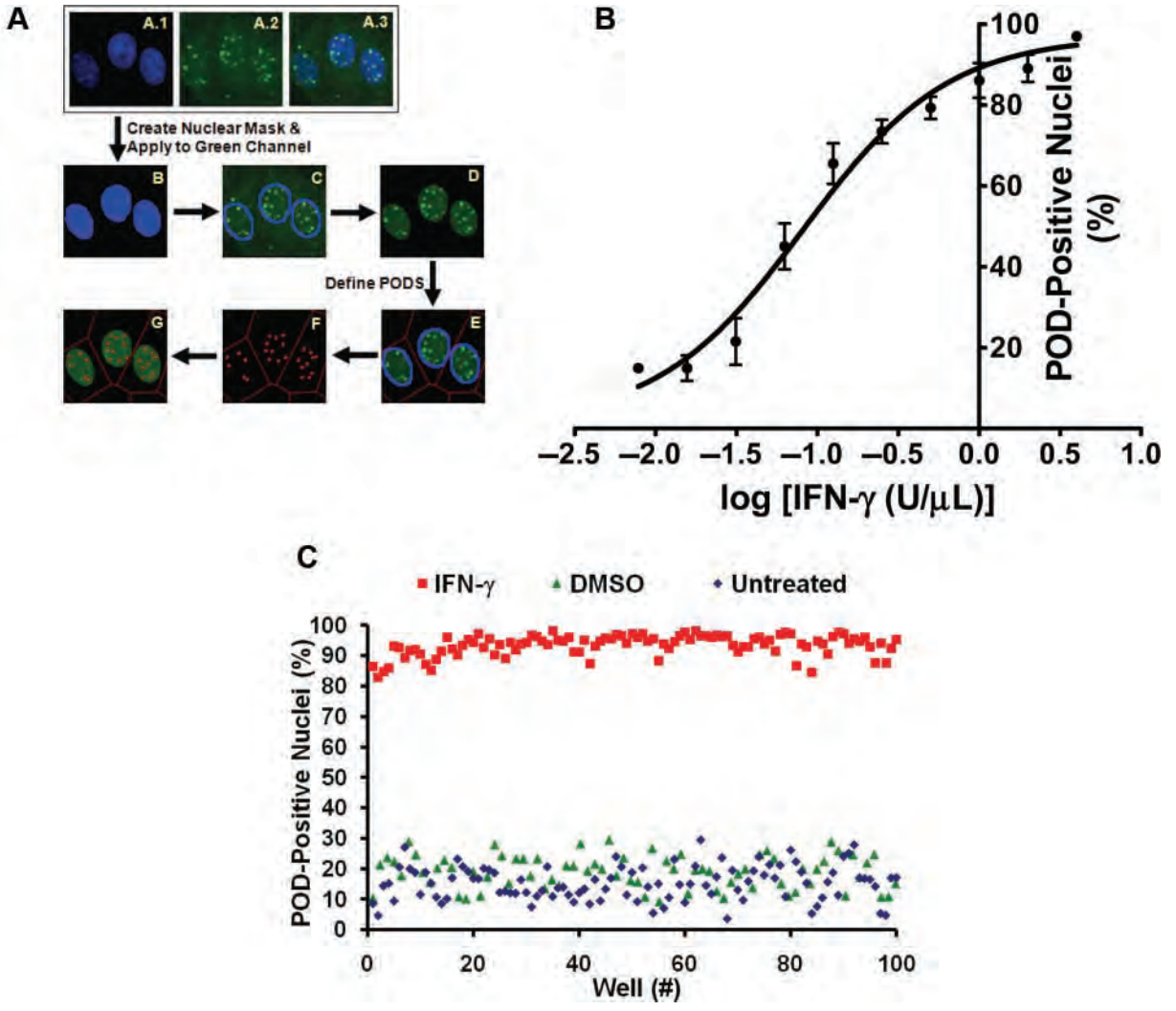

FIG. 2. High-content screen (HCS) development and optimization. (**A**) Algorithm for detecting and quantifying PML oncogenic domains (PODs). DAPI (A.1; blue), PML (A.2; green), and merged (A.3) images of interferon-γ (IFN-γ)–treated (4 U/μL; 12 h) HeLa cells are shown. The nuclear (DAPI) image was used to produce a nuclear mask (B; blue). The nuclear mask (C; blue outline) was applied to the PML image. Green pixels outside of the nuclear mask were eliminated (D). Beckman Coulter CytoShop software was used to estimate cellular area (E; red outline) based on the nuclei. POD outlines (F; red) were identified based on differences in green pixel brightness. The number of detected PODs (G; red) was reported on a per nucleus basis. The percentage of POD-positive nuclei (>4.0 PODs per cell) was reported. (**B**) Quantification of IFN-γ-induced POD formation. HeLa cells were seeded in a 384-well plate (3150 cells/well) and treated with increasing concentrations of IFN-γ (12 h) as shown. Cells were immunostained for PODs (mouse monoclonal antihuman PML and Alexa Fluor 488 chicken antimouse antibodies), incubated in DAPI (nuclear stain; 100 ng/mL), imaged using the Beckman Coulter Cell Lab IC-100 Image Cytometer (40× 0.6NA ELWD Plan Fluor objective), and quantified using the described computerized algorithm. Mean ± standard deviation are shown (n = 4 wells/data point, >200 cells imaged and quantified per well). (**C**) POD HCS reproducibility assessment. HeLa cells were cultured overnight in a 384-well plate (3150 cells/well seeded using the Matrix WellMate bulk liquid dispenser; treated with IFN-γ (4 U/μL), DMSO (0.1%), or nothing for 12 h; and immunostained for PML, imaged, and analyzed (n > 85 wells/condition). The Z′ factor is 0.64 or 0.65 using DMSO or untreated cells, respectively, as the negative control.

screen large collections of compounds. This library was screened at 5 μg/mL (~10 μM for average molecular weight [MW] ≈500 g/mol) and 10 μg/mL (~20 μM for average MW ≈500 g/mol; **Fig. 3B**). The most active mixture was "1422," which induced >40% POD-positive cells.

The 1422 library contains compounds with an N-methyl triamine scaffold in which chemical diversity was created at 3 positions, R_1, R_2, and R_3. Analysis of a collection of N-methyl triamines, at which one of these diversity positions was fixed, allowing the others to vary as a mixture of all possibilities built

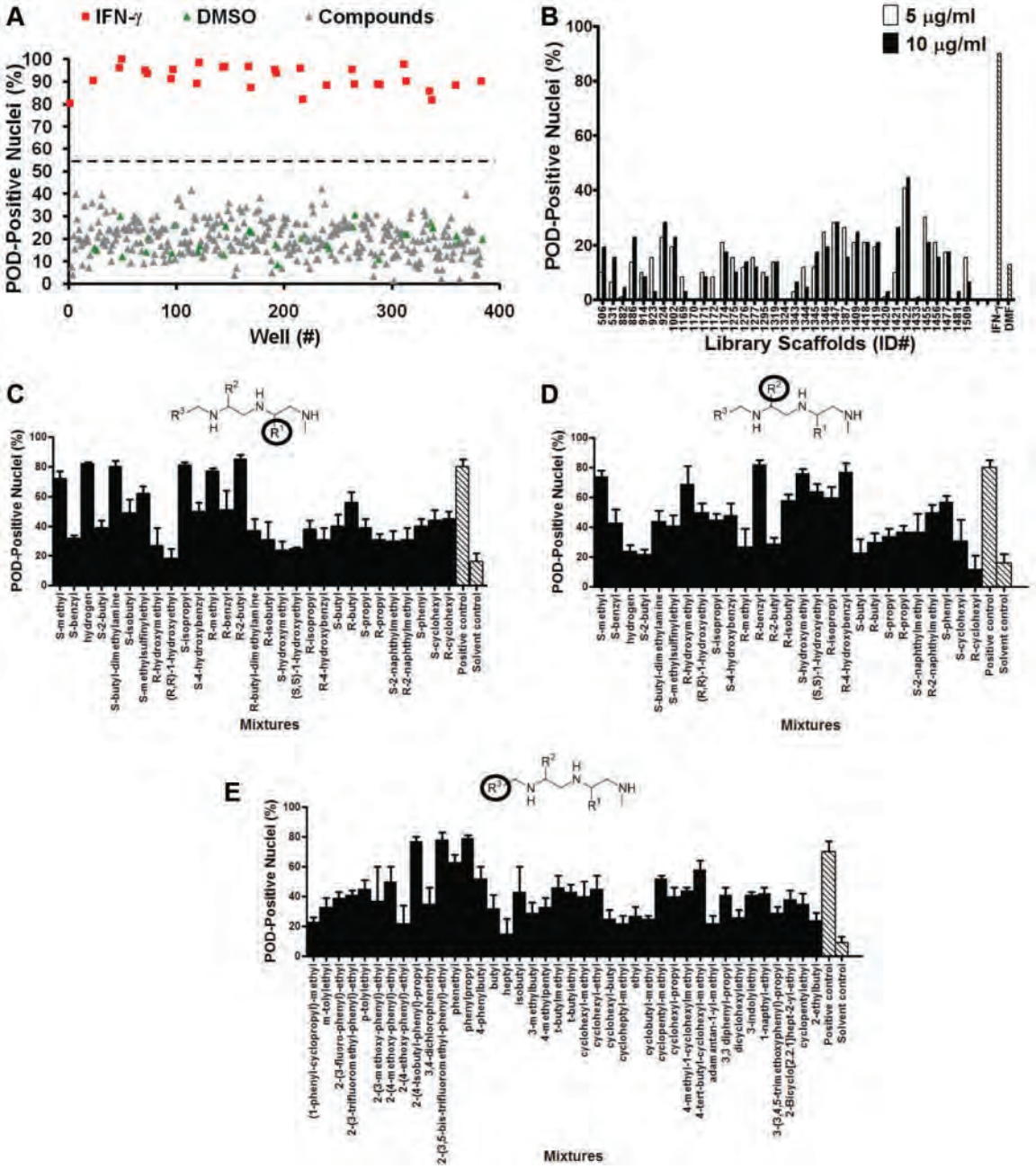

FIG. 3. High-content screening (HCS) for chemical activators of PML oncogenic domains (PODs). (**A**) Sample plate from the LOPAC[1280] POD localization screen. HeLa cells were seeded in 384-well plates (3150 cells/well) and incubated at 37 °C overnight. The cells were then treated for 12 h with IFN-γ (4 U/μL; positive control), DMSO (0.1%; negative control), or LOPAC[1280] compounds (5 μM). Plates were immunostained for PML, imaged, and analyzed. The Z′ factor was 0.55. (The dotted line represents the mean value between the positive and negative controls.) (**B**) TPIMS combinatorial library POD localization screen. Cells were screened as described previously but with mixtures from the TPIMS scaffold ranking library (5 μg/mL or 10 μg/mL, representing ~10 μM or ~20 μM, respectively, for molecular weight [MW] ≈500 g/mol). Interferon-γ (IFN-γ; 4 U/μL) was used as the positive control, and dimethylformamide (DMF; 0.1%) was used as the negative control. The Z′ factor was 0.6. (**C-E**) Combinatorial library deconvolution reveals the structure-activity relationship of N-methyl triamine compounds. Deconvolution of the mixture-based N-methyl triamine library was accomplished by the positional scanning method,[23-26] where one of the substituents used to create the library was fixed at positions (**C**) R1, (**D**) R2, or (**E**) R3, and the other positions were allowed to vary as mixtures of all possible substituents employed in library construction. Compounds were tested at 4 μg/mL (representing ~8 μM for MW ≈500 g/mol). IFN-γ (4 U/μL) was used as the positive control, and DMF (0.1%) was used as the negative control (striped bar). The Z′ factor was ~0.5.

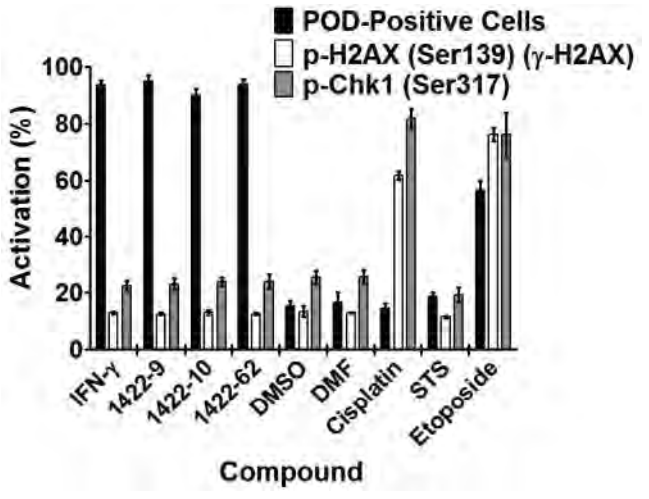

FIG. 4. PML oncogenic domain (POD)–inducing N-methyl triamines do not induce DNA damage. HeLa cells were treated for 12 h with interferon-γ (IFN-γ; 4 U/μL), DMSO (0.1%), dimethylformamide (DMF; 0.1%), cisplatin (25 μM), staurosporine (STS; 25 nM), etoposide (25 μM), or 1422 compounds (N-methyl triamines; 10 μM). Cells were then immunostained for PODs (mouse monoclonal antihuman PML, Alexa Fluor 488 chicken antimouse antibodies), phospho-H2AX (rabbit polyclonal antihuman phospho-H2AX-Ser139, Alexa Fluor 568 goat antirabbit antibodies), or phospho-Chk1 (rabbit polyclonal antihuman phospho-Chk1-Ser317, Alexa Fluor 568 goat antirabbit antibodies). POD-positive nuclei (%) were quantified as previously described. p-H2AX and p-Chk1 nuclear staining intensity was quantified using CytoShop. Mean and standard deviation are shown (n = 4 wells/condition, >200 cells imaged and quantified per well).

into the combinational library, revealed substituents at R1, R2, or R3 that induced >50% POD-positive cells when tested at 4 μg/mL (~8 μM; **Fig. 3C-E**). Successful implementation of the HCS assay for POD inducers for structure-activity relation (SAR) analysis of the N-methyl triamine combinatorial library demonstrates the robust performance of the assay.

POD-inducing specificity

To complement the HCS assay for POD activation, we also devised 2 HCS counterscreen assays using immunostaining for the DNA damage/repair–related proteins, H2AX and Chk1. H2AX is phosphorylated primarily by ATM, which "senses" double-stranded DNA breaks, whereas Chk1 is phosphorylated primarily by ATR, which "senses" single-stranded DNA breaks (a common intermediate found at sites of DNA damage detection and repair pathways).[25] Immunofluorescence staining for phospho-H2AX (Ser139) (γ-H2AX) and phospho-Chk1 (Ser317), which are visible as nuclear aggregates, was used as a counterscreen to test the specificity of the most active 1422 compounds. The similarity in antigen redistribution for H2AX and Chk1 compared to PML provides the basis for counterscreens that eliminate false-positive compounds that might affect PML or alter immunostaining patterns in a nonspecific manner. In addition, because some types of DNA-damaging agents can stimulate POD formation,[25-29] the phospho-H2AX and phospho-Chk1 immunofluorescence counterscreens serve to eliminate compounds that operate as DNA-damaging agents and thus eliminate these from further consideration.

For these counterscreen HCS assays, CytoShop algorithms were used to quantify the intensity of nuclear phospho-H2AX (Ser139) (γ-H2AX) or phospho-Chk1 (Ser317) immunofluorescence. As shown in **Figure 4** (and **Supplemental Figures S2-S4 online at http://jbx.sagepub.com/content/by/supplemental-data**), IFN-γ (POD-positivity control) induced PML localization to PODs without affecting the markers of DNA damage. Similarly, 3 active N-methyl triamine (1422) compounds synthesized based on results from the combinatorial library analysis (1422-9, 1422-10, and 1422-62) induced PML localization into nuclear aggregates without altering phospho-H2AX or phospho-Chk1, thus confirming the selectivity of their POD-inducing activity. In contrast, cisplatin (DNA damage control) induced H2AX and Chk1 phosphorylation without affecting POD formation, whereas etoposide (DNA damage control) simultaneously induced POD formation, H2AX phosphorylation, and Chk1 phosphorylation. Staurosporine (a broad-spectrum kinase inhibitor), DMSO (solvent control), and DMF (solvent control) had little effect on POD activation, H2AX phosphorylation, or Chk1 phosphorylation. Altogether, these results validate both the primary HCS assay for detection of POD activators and also the counterscreening assays for elimination of DNA damage-inducing compounds.

DISCUSSION

The current study describes an HCS assay for compounds that induce PML to localize to PODs, subnuclear structures involved in a variety of tumor-suppressive pathways, and host defense against some types of viruses. After developing algorithms for automated analyses of POD formation, the LOPAC^{1280} and TPIMS combinatorial libraries were screened. No hits were identified among the 1280 pharmacologically active LOPAC^{1280} compounds, possibly providing evidence that the HCS assay is highly specific and does not suffer from promiscuous reactivity. Screening of the TPIMS combinatorial libraries, which consist of mixtures representing 5,287,896 compounds and several million peptides, revealed a bioactive N-methyl triamine mixture. Further SAR evaluations where library deconvolution was performed by the positional scanning method revealed a clear SAR and thus validated the HCS assay for detection of POD-inducing compounds. Furthermore, N-methyl triamines that were active in the POD assay did not affect the distribution of control proteins, H2AX and Chk1, demonstrating specificity.

Some types of DNA damage have been shown to induce the formation of PML-type bodies that are thought to be functionally

different from the tumor-suppressive and antiviral PODs mentioned in the current study.[25-29] Thus, the HCS counterscreen assays described here eliminate DNA-damaging compounds from further consideration.

Active compounds such as the N-methyl triamines could potentially induce PODs via several different mechanisms. First, IFN-α, -β, and -γ induce POD formation by upregulating PML and various POD-associated proteins.[9] Thus, compounds might induce interferon production, a mechanism that can be readily determined by measuring interferon elaboration into culture supernatants (e.g., using immunoassays) or by testing activation of interferon-inducible reporter genes (e.g., ISGE-luciferase). Second, arsenicals have been shown to activate PML by directly conjugating cysteines within the zinc fingers of the PML RBCC domain,[30] and thus compounds that covalently modify these sites define an additional mechanism for POD activation. Third, conjugation of PML by the ubiquitin-like protein SUMO is required for POD formation.[31] Hence, compounds that affect SUMOylation represent another potential mechanism, which might include, for instance, inhibitors of the proteases responsible for de-SUMOylation. Finally, PML binding proteins such as Daxx are regulated by phosphorylation.[32] The protein kinase ZIPK, for example, has been shown to be required for interferon to induce POD formation.[28] Thus, compounds that influence the relevant kinases or phosphatases represent another potential class of POD activators that might be revealed by our HCS assay.

Because of the role of PODs in tumor suppression and host defense against viruses, POD-inducing compounds may have relevance to a wide variety of cancers and infectious diseases. Arsenicals are already being used to treat leukemias (such as APL) and multiple myeloma.[2,16] In addition, adenoviruses, herpes simplex virus–1, human cytomegalovirus, Epstein-Barr virus, papillomavirus, hepatitis D virus, human T-lymphotropic virus–1, lymphocytic choriomeningitis, and rabies viruses disrupt PODs,[9] suggesting that POD-inducing compounds may also promote antiviral states that could be therapeutically useful. The HCS assay described here enables high-throughput screening (HTS) for compounds with potential medicinal activity based on induction of PODs, thus providing a route to chemical modulators of PML that accommodates the diversity of cellular mechanisms responsible for POD regulation in a manner unachievable with standard biochemical HTS assays.

ACKNOWLEDGMENTS

We thank Tessa Siegfried and Melanie Hanaii for assistance with manuscript preparation, as well as Drs. Paul Diaz and Satoshi Ogasawara for technical assistance. Support by DoD grant W81XWH-08-0574 and NIH grant CA-55164.

REFERENCES

1. Bernardi R, Pandolfi PP: Structure, dynamics and functions of promyelocytic leukaemia nuclear bodies. *Nat Rev Mol Cell Biol* 2007;8:1006-1016.
2. Salomoni P, Pandolfi PP: The role of PML in tumor suppression. *Cell* 2002;108:165-170.
3. Melnick A, Licht JD: Deconstructing a disease: RARalpha, its fusion partners, and their roles in the pathogenesis of acute promyelocytic leukemia. *Blood* 1999;93:3167-3215.
4. Wang ZG, Ruggero D, Ronchetti S, Zhong S, Gaboli M, Rivi R, et al: PML is essential for multiple apoptotic pathways. *Nat Genet* 1998;20:266-272.
5. Wang ZG, Delva L, Gaboli M, Rivi R, Giorgio M, Cordon-Cardo C, et al: Role of PML in cell growth and the retinoic acid pathway. *Science* 1998;279:1547-1551.
6. Salomoni P, Bernardi R, Bergmann S, Changou A, Tuttle S, Pandolfi PP: The promyelocytic leukemia protein PML regulates c-Jun function in response to DNA damage. *Blood* 2005;105:3686-3690.
7. Hofmann TG, Will H: Body language: the function of PML nuclear bodies in apoptosis regulation. *Cell Death Differ* 2003;10:1290-1299.
8. Jensen K, Shiels C, Freemont PS: PML protein isoforms and the RBCC/TRIM motif. *Oncogene* 2001;20:7223-7233.
9. Regad T, Chelbi-Alix MK: Role and fate of PML nuclear bodies in response to interferon and viral infections. *Oncogene* 2001;20:7274-7286.
10. Guo A, Salomoni P, Luo J, Shih A, Zhong S, Gu W, et al: The function of PML in p53-dependent apoptosis. *Nat Cell Biol* 2000;2:730-736.
11. Song MS, Salmena L, Carracedo A, Egia A, Lo-Coco F, Teruya-Feldstein J, et al: The deubiquitinylation and localization of PTEN are regulated by a HAUSP-PML network. *Nature* 2008;455:813-817.
12. Puto LA, Reed JC: Daxx represses RelB target promoters via DNA methyltransferase recruitment and DNA hypermethylation. *Genes Dev* 2008;22:998-1010.
13. Croxton R, Puto LA, de Belle I, Thomas M, Torii S, Hanaii F, et al: Daxx represses expression of a subset of antiapoptotic genes regulated by nuclear factor-kappaB. *Cancer Res* 2006;66:9026-9035.
14. Zhong S, Hu P, Ye TZ, Stan R, Ellis NA, Pandolfi PP: A role for PML and the nuclear body in genomic stability. *Oncogene* 1999;18:7941-7947.
15. Khan MM, Nomura T, Kim H, Kaul SC, Wadhwa R, Zhong S, et al: PML-RARalpha alleviates the transcriptional repression mediated by tumor suppressor Rb. *J Biol Chem* 2001;276:43491-43494.
16. Crowder C, Dahle O, Davis RE, Gabrielsen OS, Rudikoff S: PML mediates IFN-alpha-induced apoptosis in myeloma by regulating TRAIL induction. *Blood* 2005;105:1280-1287.
17. Berenson JR, Yeh HS: Arsenic compounds in the treatment of multiple myeloma: a new role for a historical remedy. *Clin Lymphoma Myeloma* 2006;7:192-198.
18. Dunn GP, Ikeda H, Bruce AT, Koebel C, Uppaluri R, Bui J, et al: Interferon-gamma and cancer immunoediting. *Immunol Res* 2005;32:231-245.
19. Houghten RA, Pinilla C, Appel JR, Blondelle SE, Dooley CT, Eichler J, et al: Mixture-based synthetic combinatorial libraries. *J Med Chem* 1999;42:3743-3778.
20. Pinilla C, Appel JR, Blanc P, Houghten RA: Rapid identification of high affinity peptide ligands using positional scanning synthetic peptide combinatorial libraries. *Biotechniques* 1992;13:901-905.
21. Pinilla C, Appel JR, Borras E, Houghten RA: Advances in the use of synthetic combinatorial chemistry: mixture-based libraries. *Nat Med* 2003;9:118-122.
22. Zhang JH, Chung TD, Oldenburg KR: A simple statistical parameter for use in evaluation and validation of high throughput screening assays. *J Biomol Screen* 1999;4:67-73.
23. Kawai T, Akira S, Reed JC: ZIP kinase triggers apoptosis from nuclear PML oncogenic domains. *Mol Cell Biol* 2003;23:6174-6186.

24. Houghten RA, Pinilla C, Giulianotti MA, Appel JR, Dooley CT, Nefzi A, et al: Strategies for the use of mixture-based synthetic combinatorial libraries: scaffold ranking, direct testing in vivo, and enhanced deconvolution by computational methods. *J Comb Chem* 2008;10:3-19.
25. Sancar A, Lindsey-Boltz LA, Unsal-Kacmaz K, Linn S: Molecular mechanisms of mammalian DNA repair and the DNA damage checkpoints. *Annu Rev Biochem* 2004;73:39-85.
26. Eskiw CH, Dellaire G, Mymryk JS, Bazett-Jones DP: Size, position and dynamic behavior of PML nuclear bodies following cell stress as a paradigm for supramolecular trafficking and assembly. *J Cell Sci* 2003;116:4455-4466.
27. Zhong S, Salomoni P, Ronchetti S, Guo A, Ruggero D, Pandolfi PP: Promyelocytic leukemia protein (PML) and Daxx participate in a novel nuclear pathway for apoptosis. *J Exp Med* 2000;191:631-640.
28. Seker H, Rubbi C, Linke SP, Bowman ED, Garfield S, Hansen L, et al: UV-C-induced DNA damage leads to p53-dependent nuclear trafficking of PML. *Oncogene* 2003;22:1620-1628.
29. Tanaka T, Halicka HD, Traganos F, Seiter K, Darzynkiewicz Z: Induction of ATM activation, histone H2AX phosphorylation and apoptosis by etoposide: relation to cell cycle phase. *Cell Cycle* 2007;6:371-376.
30. Zhang XW, Yan XJ, Zhou ZR, Yang FF, Wu ZY, Sun HB, et al: Arsenic trioxide controls the fate of the PML-RARalpha oncoprotein by directly binding PML. *Science* 2010;328:240-243.
31. Shen TH, Lin HK, Scaglioni PP, Yung TM, Pandolfi PP: The mechanisms of PML-nuclear body formation. *Mol Cell* 2006;24:331-339.
32. Salomoni P, Khelifi AF: Daxx: death or survival protein? *Trends Cell Biol* 2006;16:97-104.

Address correspondence to:
Dr. John C. Reed
Sanford-Burnham Medical Research Institute
10901 North Torrey Pines Road, La Jolla, CA 92037

E-mail: reedoffice@sanfordburnham.org